RACK1 stabilises the activity of PP2A to regulate the transformed phenotype in mammary epithelial cells.

Maeve Kiely[1], David R. Adams[2], Sheri L. Hayes[1], Rosemary O'Connor[3], George S. Baillie[4], Patrick A. Kiely[1*]

[1] *Graduate Entry Medical School, Materials and Surface Science Institute and Health Research Institute, University of Limerick, Ireland.*
[2] *Institute of Chemical Sciences, Heriot-Watt University, Riccarton Campus, Edinburgh EH14AS, UK.*
[3] *Cell Biology Laboratory, Department of Biochemistry, BioSciences Institute, University College Cork, Cork, Ireland*
[4] *Institute of Cardiovascular & Medical Science, College of Medical, Veterinary & Life Sciences, University of Glasgow, Glasgow G12 8QQ, UK.*

***Corresponding author:**
Dr Patrick A. Kiely,
Graduate Entry Medical School,
University of Limerick, Limerick,
Ireland.
Patrick.Kiely@ul.ie

Highlights

RACK1 scaffolds active PP2A.

RACK1 stabilises PP2A activity.

RACK1/PP2A complex is required for cell adhesion, proliferation, migration, invasion.

Potential role for the RACK1/PP2A complex in the progression of breast cancer.

Keywords

Breast Cancer, RACK1, PP2A, Protein-Protein Interactions.

Abbreviations.

Cell Index (CI), Epidermal Growth Factor (EGF), Focal Adhesion Kinase (FAK), Insulin-like Growth Factor-1 (IGF-1), Leucine carboxyl methyltransferase 1 (LCMT-1), Mitogen Activated Protein (MAP) kinase, Phosphodiesterase 4D5 (P4DED5), Protein Phosphatase 2A (PP2A), Receptor for Activated C Kinase (RACK1), Wild Type (WT),

ABSTRACT

Conflicting reports implicate the scaffolding protein RACK1 in the progression of breast cancer. RACK1 has been identified as a key regulator downstream of growth factor and adhesion signalling and as a direct binding partner of PP2A. Our objective was to further characterise the interaction between PP2A and RACK1 and to advance our understanding of this complex in breast cancer cells. We examined how the PP2A holoenzyme is assembled on the RACK1 scaffold in MCF-7 cells. We used immobilized peptide arrays representing the entire PP2A-catalytic subunit to identify candidate amino acids on the C subunit of PP2A that might be involved in binding of RACK1. We identified the RACK1 interaction sites on PP2A. Stable cell lines expressing PP2A with FR69/70AA, R214A and Y218F substitutions were generated and it was confirmed that the RACK1/PP2A interaction is essential to stabilize PP2A activity. We used Real-Time Cell Analysis and a series of assays to demonstrate that disruption of the RACK1/PP2A complex also reduces the adhesion, proliferation, migration and invasion of breast cancer cells and plays a role in maintenance of the cancer phenotype. This work has significantly advanced our understanding of the RACK1/PP2A complex and suggests a pro-carcinogenic role for the RACK1/PP2A interaction. This work suggests that approaches to target the RACK1/PP2A complex are a viable option to regulate PP2A activity and identifies a novel potential therapeutic target in the treatment of breast cancer.

1. **Introduction**

RACK1 plays a critical role in many fundamental cellular processes including cell adhesion, proliferation, migration and protein synthesis through its ability to act as a scaffold within signalling pathways [1-4]. RACK1 is known to interact with a diverse array of proteins and functions to recruit and shuttle these proteins to their substrates or other binding partners [1, 2]. Alterations in RACK1 expression and function are associated with a variety of disease states including Alzheimer's disease [5], bipolar disorder [6] and cancer including hepatocellular carcinoma, ovarian cancer and cancers of the prostate and breast [7-11]. The connection between RACK1 and cancer is complex, since RACK1 interacts with over 80 binding partners, either directly or indirectly in large complexes, thereby impacting on multiple signalling pathways. Many of the proteins in the RACK1 interactome are phosphatases and kinases whose activity is altered in cancer. For example, RACK1 plays a critical part in cell adhesion and migration, in particular through its role in regulating focal adhesion kinase (FAK) activity and focal adhesion assembly [12, 13]. RACK1 is also a component of the signalling pathways downstream of FAK and phosphodiesterase 4D5 (PDE4D5) that control both cell spreading and the direction sensing mechanisms required to establish cell polarity, which is an important element in the process of cell migration [14, 15]. RACK1 has also been shown to promote both cell migration and invasion in both oesophageal and lung cancers through a variety of different signalling mechanisms [16-18].

Conflicting reports suggest a role for RACK1 in breast cancer. High RACK1 expression has been reported in breast cancer patients, and this has been correlated with a poor clinical outcome [10]. RACK1 has also been found to promote breast cancer proliferation and invasion both *in vitro* and in mouse models through interaction with RhoA and activation of the RhoA/Rho kinase pathway [19]. This suggests that RACK1 has potential as a valuable prognostic indicator of advanced disease in breast cancer. However,

other studies report findings that are in direct contrast to this. For example, decreased RACK1 is reported in a cohort of breast cancer patients and associated with a good clinical outcome in follow-up studies [11]. This apparent conflict in findings of RACK1 expression in cancer tissue could be due to the heterogeneous nature of breast cancer and the inconsistencies may be explained by a lack of information on breast cancer subtypes within these studies [20]. Also, because RACK1 is involved in the scaffolding of such a large number of proteins within such diverse signalling pathways, it is acknowledged that any change in RACK1 expression, either up or down, has the potential to have serious consequences for the tight regulation of these pathways and as a result, on the processes regulating the establishment, development and progression of cancer [1].

Protein Phosphatase 2A (PP2A) is a major Ser/Thr phosphatase in cell signalling pathways. PP2A exists as a holoenzyme with three individual components. Once assembled, the structural subunit (A) and catalytic subunit (C) form the core dimer while the regulatory subunit (B) confers substrate specificity, full activity and subcellular location of the PP2A holoenyme when bound to the core dimer. There are two A isoforms (α and β) which share 87% sequence homology and two C subunits (α and β) which share 97% homology [21-23]. Currently, there are up to 26 known regulatory B subunits [24]. As a phosphatase, PP2A is essential to promote the post translational modifications that reverse kinase activity in many of the major cell signalling pathways, including those that regulate the cell cycle, metabolism, cell migration and survival [24-27]. It is also widely accepted that PP2A negatively regulates growth factor signalling and MAP kinase activation downstream of growth factor signalling [28, 29].

PP2A directly interacts with RACK1 in an IGF-1 dependent manner where RACK1 serves to stabilise PP2A activity [30, 31]. A reduction in RACK1 expression decreases the phosphatase activity of PP2A, which has been shown to promote cell migration in cancer

cells [31]. This indicates that RACK1 has a role to play in keeping a specific pool of PP2A 'active' and thus facilitating the regulatory role of PP2A.

PP2A has a well-established role in cancer. It is largely recognised as a tumour suppressor and has been found to be mutated in many cancer types [27, 32-34]. However, inhibition of PP2A has shown potential as an anti-cancer strategy in some cell models [23, 35-38]. This apparent contradiction may arise, in part, because PP2A inhibition increases tumour chemo-sensitivity to many chemotherapeutic drugs (reviewed in [39]) but also because PP2A has been shown to play an anti-apoptotic role within signalling pathways (reviewed in [23]).

Here, we further characterise the RACK1/PP2A interaction in breast cancer cells by identifying and mapping the interaction site of RACK1 on the catalytic (C) subunit of PP2A (PP2A-C). Using mutations of PP2A that disrupt the binding with RACK1, we show that RACK1 stabilizes PP2A activity and regulates the transformed phenotype in breast cancer.

2. Materials and Methods.

2.1 Cell Culture

MCF-7 and HEK cells were maintained in DMEM supplemented with 5% L-glutamine, 5% penicillin/streptomycin and 10% FBS (Sigma-Aldrich Ltd).

2.2 Preparation of cellular protein extracts

Cellular protein extracts were prepared by placing cells on ice, removing media and washing three times in ice cold PBS. Cells were scraped into ice cold lysis buffer (20mM Tris HCl pH 7.4, 50mM NaCl, 50mM NaF, 1% NP40) plus the tyrosine phosphatase inhibitor Na_3VO_4 (1mM), protease inhibitors PMSF (1mM), pepstatin (1µM) and aprotinin (1.5µg/ml). Lysates were incubated on ice for 20 minutes before centrifugation at 14,000 rpm for 15 minutes at 4ºC to remove nuclei and cellular debris. Lysates were analysed for protein concentration using the Bradford assay and boiled in sample buffer for SDS-PAGE or used in immunoprecipitation experiments.

2.3 Immunoprecipitation of proteins and Western Blotting

Protein extracts were precleared with 20µl Protein G beads by incubation at 4ºC for 1 hour rotating. The lysates were recovered from the beads by centrifugation at 3,000 rpm for 3 minutes and transferred to a new tube containing primary antibody (2µg), 40µl Protein G beads, 500µl lysis buffer and made up to 1ml with dH_2O. Samples were incubated at 4ºC rotating overnight. Immune complexes were pelleted with the beads by centrifugation at 3,000 rpm for 3 minutes at 4 ºC. The beads were washed three times with ice cold lysis buffer and removed from beads by boiling for 5 minutes in 25µl of 2x SDS PAGE sample buffer for electrophoresis and western blot analysis. Protein samples for western blot analysis were separated by 12% SDS-PAGE gels. Following separation on the gel, proteins were transferred using electrophoresis onto a nitrocellulose membrane and blocked for 1 hour at

room temperature shaking in 5% milk (w/v) in TBS containing 0.5% Tween-20 (TBS-T). Membranes were incubated overnight at 4ºC with the appropriate primary antibody; Anti-PP2A-Cα subunit (Cell Signalling), Anti-RACK1 (BD Biosciences). Appropriate secondary antibodies (IRDye® 680LT and 800CW- Infrared Dye coupled anti-rabbit or anti-mouse (LI-COR Biosciences)) were diluted 1:10000 in TBS-T/5% milk for 1 hour. Antibody reactive bands were detected with the Odyssey® infrared imaging system (LI-COR Biosciences).

2.4 Spot Synthesis of peptides, overlay analysis and alanine substitution array analysis

Peptide arrays of PP2A-C on nitrocellulose were generated as previously described [40-42]. Scanning libraries of overlapping 23-mer peptides covering the entire sequence of a protein were produced by automatic SPOT synthesis and synthesized on Whatman 50 cellulose using Fmoc (9-fluorenylmethyloxycarbonyl) chemistry with the AutoSpot-Robot ASS 222 (Intavis Bioanalytical Instruments). The interaction of GST and GST-tagged proteins, e.g. GST-RACK1 with the protein array was investigated by overlaying the cellulose membranes with 10 μg/ml concentrations of each recombinant protein. Bound protein was detected with specific mouse antisera for each protein and a secondary anti-mouse antibody coupled with LICOR dye 680 and scanned on the Odyssey Infrared Scanner. Once candidate binding regions for RACK1 on the full-length PP2A-C subunit array had been determined, specific alanine scanning substitution arrays were generated for the relevant sequences using the same synthesis procedure. The progeny peptide arrays were synthesized in 18-mer format such that each of the 18 amino acids of the PP2A-C sequence were sequentially substituted with alanine (or aspartic acid where the wild-type sequence exhibited alanine). The array was probed with GST-RACK1 at a concentration of 10μg/ml, which was detected by immunoblotting with anti-RACK1 antibody. Bound protein was detected with specific mouse antisera for the protein and a secondary anti-mouse antibody coupled with LICOR dye 680 and scanned on the Odyssey Infrared Scanner. A decrease in intensity in binding to the

peptides after alanine substitution is indicative of decreased binding of the PP2A-C subunit to RACK1. The binding of RACK1 to each alanine-substituted PP2A-C subunit peptide was quantified by densitometry and presented as a percentage of the control ‘‘parent’’ sequence. A cut off of less than 50% binding was applied.

2.5 Generation of stable cell lines

To generate stable transfectants of PP2A mutants, MCF-7 cells were transfected with pcDNA3/HA-Empty Vector, pcDNA3/HA-PP2A (Wild Type), pcDNA3/HA-FR69/70AA, pcDNA3/HA-R214A and pcDNA3/HA-Y218F using Lipofectamine 2000 transfection reagent. Then, 24 hours post transfection, the cells were split into DMEM medium containing 10% FBS, 10mM l-glu and G418 (1mg/ml) and maintained for 14 days, with regular replenishment of medium and drug. At this time the pool was expanded, and screened for expression of the HA tagged plasmids by Western blotting. Clones of MCF-7 cells stably overexpressing the plasmids were maintained in DMEM supplemented with 1 mg/ml G418.

2.6 PP2A Phosphatase Activity Assay

Cellular PP2A activity was measured using threonine phosphopeptide as the substrate with the PP2A immunoprecipitation phosphatase assay kit (Millipore). Cells were washed with PBS before being lysed using a lysis buffer (20mM imidazole-HCL, 2mM EDTA, 2mM EGTA, pH 7.0 with 10µg/ml aprotinin and 1mM PMSF). Cells were sonicated for 10 seconds and centrifuged at 2000g for 5 min. Clarified supernatants were incubated with anti- HA antibody (4µg) with protein A agarose slurry for 18 h at 4º with gentle rocking. Beads were washed 3 times with 700µl TBS, and once with 500µl Ser/Thr assay buffer. The beads were then incubated with 60µl diluted phosphopeptide and 20µl Ser/Thr assay buffer at 30ºC for 10 min in a shaking incubator. The beads were centrifuged briefly and the samples were analysed in a colorimetric assay using malachite green at an absorbance of 650 nm.

2.7 Cell adhesion, spreading, proliferation and invasion using the RTCA xCELLigence system

Cells were harvested with trypsin/EDTA, washed with DMEM, and re-suspended in the DMEM with 10% FBS. The cells were counted using a haemocytometer. Cells were seeded in each well of the E-plate. The impedance values of each well were automatically monitored by the xCELLigence system and expressed as a cell index value (CI). The baseline impedance is recorded using control wells containing DMEM only with no cells. Unless otherwise stated, cells were seeded onto the E-plate at a density of 20,000 per well. The E-plate was then placed into the xCELLigence system. Scans were run with sweeps every minute for the first eight hours to detect early stages of cell adhesion and spreading. Subsequent sweeps were taken every 15 minutes for the duration of the 48 hour experiment to examine proliferation.

2.8 Adhesion Assay

Collagen plates were prepared by coating wells of a 96 well plate with 100µl of 10µg/ml collagen I. The plates were incubated at 4°C overnight or alternatively incubated at 37°C for 2-3 hours. The wells were washed twice with PBS and blocked with 50µl PBS/2.5% BSA and incubated at 37° for 1-2 hours. Cells were washed 3 times with PBS. 2000 cells were plated into the pre-prepared wells and incubated at 37°C in 5% CO_2 for 1 hour. Then, cells were washed 3 times with PBS and fixed in 100µl methanol at -20°C for 5 minutes. The methanol was removed and cells were stained with 0.1% crystal violet for 15 minutes at room temperature. Cells were carefully washed with water and left overnight to dry. The plates were then read at 590 nm on a spectrophotometer.

2.9 Migration Assay

Plastic culture inserts (Ibidi®) with an adhesive bottom layer were placed into wells of a 24 well plate. 20,000 cells were plated into the wells containing the inserts. The cells were left overnight to adhere fully. The insert was removed which leaves a cell free gap of 500µm ± 50µm. The cells were photographed using a Nikon microscope with a x63 lens at 0 hours and 24 hours. The migration of cells was analysed using Ibidi® Quantitative Image Analysis.

2.10 Cell invasion using the RTCA xCELLigence system.

Cell invasion was monitored in real-time with the xCELLigence system CIM-plates. 4 hours prior to conducting the experiment the PP2A stable mutant cells were serum starved. The upper chamber of the CIM plates was coated with 1 µg/µl of fibronectin and a 1:40 solution of Matrigel^{TM}. A total of 20,000 cells were seeded in each well of the upper chamber in serum-free media. DMEM media containing 10% FBS was added to each well of the lower chamber. The CIM-plate was left in an incubator for 1 hour to allow cell attachment. The impedance value of each well was automatically monitored by the xCELLigence system for duration of the experiment and expressed as a CI value.

2.11 Plating Efficiency Assay

The stable PP2A mutant cell lines were harvested with trypsin/EDTA, washed with DMEM and counted using a haemocytometer. 500 cells of each were plated per well of a 6 well plate. The plates were incubated at 37° in 5% CO_2 for 10 days. After 10 days, the cells were fixed in 96% ethanol for 10 min and subsequently stained with 0.05% crystal violet (made in 20% ethanol) for 20 min. The wells were washed carefully in trays of water and allowed to dry. Colonies were counted and recorded. A colony was deemed to be of 50 cells or more in size. This was done in triplicate.

2.12 Soft Agar Assay

Wells were coated with a 0.6% agarose layer which was made in DMEM with 10% FBS. This was left for 20 minutes to allow the agarose to solidify. The stable PP2A mutant cell lines were harvested with trypsin/EDTA, washed with DMEM, and re-suspended in the DMEM with 10% FBS containing 0.3% agarose. The cells were counted using a haemocytometer and plated in quadruplicate. The cells were overlaid very carefully with DMEM with 10% FBS. Cells were left to incubate for 14 days. Colonies were then stained with 0.01% crystal violet overnight and counted using a light microscope which aids in creating contrast.

2.13 Statistics

All statistics were done using SPSS 20 Statistical Package. Data is presented as mean ± standard error of the mean (SEM) unless otherwise stated. Differences were determined using Mann-Whitney (activity assay) or student t-test and differences between groups were determined using one-way ANOVA with multiple groups compared using Bonferroni correction. A *P* value less than 0.05 was considered statistically significant.

3. Results.

3.1 Mapping the interaction between RACK1 and the PP2A-C subunit.

We have previously established that PP2A competes with β1 integrin for binding to WD7 of RACK1 and that the binding was regulated by IGF-I and required for IGF-I-mediated cell adhesion [30, 31]. We set out to further characterise the interaction between RACK1 and the PP2A holoenzyme. We first confirmed that RACK1 is in a complex with the PP2A-C subunit. RACK1 was immunoprecipitated from MCF-7 cells. The RACK1 IP was analysed for associated HA-tagged PP2A-C by western blotting. In the reciprocal experiment, PP2A-C was immunoprecipitated and analysed for associated RACK1 by western blotting, and the RACK1 and PP2A-C complex was confirmed (**Fig. 1a (i)** and **(ii)**).

To refine the binding site of RACK1 on PP2A-C, we employed peptide array technology to identify the potential binding sites. Peptide arrays of immobilised overlapping 23-mer peptides, each shifted to the right by 5 amino acids encompassing the entire PP2A-C sequence were generated as previously described [12, 31, 43]. Arrays were probed with GST alone or GST-RACK1, and bound GST was detected by immunoblotting with anti-GST antibody as described in Materials and Methods (**Fig. 1b**). Positively interacting peptides generated dark spots and non-interacting peptides left blank spots. Two areas of positive binding were identified encompassing peptide spots A12-A15 and C9-C13 (**Fig. 1b**).

Next, we generated a series of alanine substitution arrays derived from the 23-mer parent peptides that identified positive on the array. For each parent peptide, 18 progeny peptides were generated such that each new peptide in the array had a single alanine substitution introduced for successive amino acids in the sequence (or aspartic acid where the wild-type residue is already alanine) (**Fig. 2a**). The alanine substitution peptide arrays were then probed with recombinant GST-RACK1 which was detected by immunoblotting with anti-GST antibody. A decrease in intensity in binding to the peptides after alanine

substitution is indicative of decreased binding of PP2A-C to RACK1. The binding of RACK1 to each alanine-substituted PP2A-C peptide was quantified by densitometry and presented as a percentage of the control ‘‘parent’’ sequence. A cut off of less than 50% binding was applied to identify those amino acids important in the interaction.

Results showed that RACK1 binding to these peptides was either severely attenuated or ablated by substituting phenylalanine 69 (F69), arginine 70 (R70), arginine 214 (R214) or tyrosine 218 (Y218) (**Fig. 2a**). In contrast, interaction between the GST-RACK1 probe and progeny peptides appeared to be enhanced in cases of alanine substitution for aspartic or glutamic acids (E67, D77, D223, E226) (**Fig. 2a**). These results suggested that the detection of array peptide binding to RACK1 might be biased towards cationic and hydrophobic sequences, thus requiring careful validation of any residues implicated in order to eliminate potentially artefactual associations. To this end, we first examined the available crystal structures of the PP2A catalytic subunit and its holoenzyme complexes (PDB: 2NPP, 2NYL, 2NYM [44]; 2IAE [45]; 3DW8 [46]; 3FGA [47]; 4I5N, 4I5L[48] in order to assess whether F69, R70, R214 and Y218 might be accessible in the intact protein and so contribute to a potential RACK1 binding site. This revealed that F69 and R70 are indeed exposed, on a heavily contoured surface proximal to the interface between the PP2A catalytic and scaffolding subunits of the holoenzyme, while R214 and Y218 are similarly surface exposed but on the opposite face of PP2A-C at or near the catalytic centre (**Fig. 2b (i)** and **(ii)**).

The guanidinium group of R214 is positioned adjacent to the catalytic metal ions in the activated PP2A-C protein and plays a dual role both as part of the substrate binding site, directly binding to phosphorylated substrates, and in stabilising a loop conformation adjacent to the catalytic site. As such, protein binding to this residue might at first sight be expected to inhibit PP2A function, and indeed the tumor-inducing toxins, okadaic acid and microcystin-LR, directly engage R214 when binding to PP2A in an inhibitory capacity [49]. However,

R214 is also known to play a role in binding proteins that facilitate activation of PP2A and holoenzyme assembly. Thus, PP2A holoenzyme assembly is a highly regulated process that involves activation of the conformationally flexible PP2A-C subunit by an ATP-dependent chaperone protein, PP2A phosphatase activator (PTPA) [50, 51] and by C-terminal carboxyl methylation, mediated by leucine carboxyl methyltransferase 1 (LCMT-1) [52-54]. Both PTPA-ATP and LCMT-1 directly engage R214 as a pivotal residue in their associations with PP2A-C.

Y218 is located quite close to the catalytic pocket and interestingly, in one crystal structure (PDB: 3FGA [47]), Y218 forms part of the surface contact for a helical fragment derived from the shugoshin protein, Sgo1, which facilitates recruitment of PP2A to centromeric cohesion [47, 55] . Although it is not thought that the interaction between RACK1 and PP2A mimics this interaction precisely (because RACK1 is unlikely to reorganise so as to present a helical motif), the observed complex between PP2A-C and Sgo1 does establish a precedent for Y218 as part of a binding surface for a partner protein. Taken together, these analyses confirm the binding of RACK1 to PP2A-C and identify key amino acids that may be required for binding of the two proteins.

3.2 Disrupting the RACK1/PP2A interaction decreases the phosphatase activity of PP2A.

Having determined putative interaction sites for RACK1 on the PP2A-C subunit, we used MCF-7 breast cancer cells to generate stable cell lines expressing HA-tagged PP2A-C with residue substitutions at the candidate RACK1 binding sites together with appropriate controls. HA-Empty Vector, HA-PP2A WT, HA-PP2A FR69/70AA, HA-PP2A R214A and HA-PP2A Y218F were transfected into the MCF-7 breast cancer cell line and transfected cells were selected and maintained using media containing the selection agent G418 (**Fig. 2c**). HA-PP2A FR69/70AA had no effect on the binding of PP2A to RACK1 (**Fig. 2c**);

however, HA-PP2A R214A and HA-PP2A Y218F were deficient in binding to RACK1 in comparison to HA-PP2A WT (**Fig. 2c**). The deficiency in HA-PP2A R214A and HA-PP2A Y218F binding to RACK1 was also confirmed by using HA-Empty Vector, HA-PP2A WT, HA-PP2A R214A and HA-PP2A Y218F to transiently transfect HEK cells. The cells were lysed and a RACK1 IP was performed and analysed for associated HA-tagged PP2A-C mutants by western blotting (**Supplementary Fig. 1a**).

Generation of HA-tagged PP2A stable mutant cell lines allowed us to investigate whether the interaction between RACK1 and the PP2A-C subunit is required for stabilisation of PP2A activity. PP2A activity was assessed using threonine phosphopeptide as the substrate with a PP2A immunoprecipitation phosphatase assay kit. The HA-tagged PP2A mutant cell lines were lysed and a HA immunoprecipitation was performed as described in Materials and Methods. Samples were also analysed in a colorimetric (malachite green) phosphatase assay, reading the absorbance at 650nm. Our results showed that the activity of the stable HA-tagged PP2A mutant cell lines, HA-PP2A FR69/70AA, HA-PP2A R214A and HA-PP2A Y218F, was decreased by over 50% in comparison to the activity levels of cells expressing WT HA-PP2A (**Fig. 2d**).

Given the key role of R214 in substrate interaction and maintenance of the PP2A-C structure (**Fig. 2b**), we might expect that phosphatase activity for the R214A mutant would be undermined irrespective of any compromising effect on the binding of RACK1. Moreover, with this mutant, general perturbation to the conformation of the R214-containing loop as a result of alanine substitution might cause loss of RACK1 binding, as indeed observed in the IP experiments, through an indirect action (potentially also affecting the presentation of Y218). These results do not, therefore, unambiguously implicate R214 in a direct RACK1-binding capacity. In contrast, the available PP2A-C crystal structures reveal no role at all for the phenolic group of Y218 in maintaining the structure of the protein. The phenol is

orientated towards solvent and is accessible for protein binding, as seen in the Sgo1 co-crystal structure (PDB: 3FGA), where the Y218-OH serves as a hydrogen bonded bridge between glutamic acid and lysine side chains on Sgo1 [47]. Loss of RACK1 binding with the Y218F substitution and the associated reduction in phosphatase activity would thus be fully consistent with the hypothesis that RACK1 plays a role in stabilising PP2A activity in cells and that Y218 contributes to a RACK1-binding surface on PP2A-C.

3.3 The RACK1/PP2A complex is required for cell adhesion and spreading.

We next asked whether the RACK1/PP2A complex plays a role in a number of important cellular mechanisms that promote the transformed phenotype. We monitored cellular adhesion and spreading in real time using the xCELLigence system (**Fig. 3a**). Cells were seeded in each well of the E-plate at a density of 20,000 cells/well. The impedance values of each well were automatically monitored by the xCELLigence system and readings taken every 60 seconds over an 8 hour period. Readings were expressed as a cell index value (CI) and data presented as a representative graph and bar graph from the xCELLigence system, which compares the adhesion and spreading of HA-PP2A WT, HA-PP2A R214A, and HA-PP2A Y218F cells over time. The xCELLigence assays show clearly that disruption of R214 and Y218 decrease the ability of the cells to adhere. We confirmed this using a more traditional cell based adhesion assay (**Fig. 3b**). We cannot unambiguously conclude that the effects in the R214A-PP2A-C expressing cell line might not be due to intrinsic loss of catalytic function in the expressed phosphatase. However, the results with cells expressing Y218F-PP2A-C support the view that disruption of RACK1/PP2A interaction causes decreased cell adhesion and spreading when compared to the control cells overexpressing WT PP2A. Although disruption at FR/AA did alter PP2A activity levels, the HA-PP2A FR69/70AA cell line showed no difference in the ability to adhere (**Supplementary Fig. 2**).

3.4 Disruption of the RACK1/PP2A complex decreases cellular proliferation and migration.

Our next objective was to determine whether disruption of the RACK1/PP2A complex had an effect on cellular proliferation. Proliferation was monitored in real time using the RTCA xCELLigence system as described in Materials and Methods. 20,000 cells/well were plated into wells of an E-plate and impedance readings were recorded automatically every 60 seconds for the first 10 hours and every 15 minutes for the remainder of the experiment. The xCELLigence graph (**Fig. 4a (i)**) is representative of duplicate wells and n=3 experiments comparing proliferation of HA-PP2A WT, HA-PP2A R214A and HA-PP2A Y218F cells over 48 hours. A comparison of the CI over 12, 24 and 48 hours (**Fig. 4a (ii) (iii**)) shows that cells stably expressing R214A and Y218F mutant PP2A-C consistently exhibit reduced proliferative capacity compared to the wild type control.

To assess the effects on migration, we employed traditional scratch wound assays to show that HA-PP2A WT migrated faster than both HA-PP2A R214A and HA-PP2A Y218F cells (**Fig. 4b**). This indicates a role for the RACK1/PP2A complex in the fundamental process of cell migration. The role of RACK1 as a scaffolding protein involved in signalling pathways important for cell migration has been well studied [1]. This data suggests that the effects of RACK1 on cell migration are likely mediated, at least in part, by stabilising the activity of PP2A.

3.5 Cellular invasion is regulated by the RACK1/PP2A complex.

To test whether the RACK1/PP2A complex plays a role in cellular invasion, we employed the xCELLigence system CIM-plates configuration as a 3D invasion model (**Fig. 5**). To do this, prior to conducting the experiment, the cells were serum starved for 4 hours. The upper chamber of the CIM plates was coated with a 2mm layer of Matrigel^{TM} on a fibronectin coating to provide a barrier through which the cells would have to invade. 20,000 cells/well

were seeded in each well of the CIM plate upper chamber in serum-free media. DMEM media containing 10% FBS was added to each well of the lower chamber to create a gradient (as described in Materials and Methods). The impedance value of each well was automatically monitored by the xCELLigence system for duration of the experiment (72 hours) and expressed as a CI value (**Fig. 5a (i)**). Invasion was compared over 24, 36, 48, 60 and 72 hours (**Fig. 5a (ii**)). Percentage difference in cell index of HA-PP2A WT was compared to HA-PP2A R214A and HA-PP2A Y218F at 72 hours (**Fig. 5a (iii)**). In this experimental set up, the invasive potential of the cells was markedly reduced when the RACK1/PP2A complex was disrupted and it was clear that cells expressing HA-PP2A WT invaded faster than both HA-PP2A R214A and HA-PP2A Y218F cells. Again, the HA-PP2A FR69/70AA cell line showed no difference in the ability to invade (Supplementary Fig. 2).

3.6 The RACK1/PP2A complex is required for optimal plating efficiency and colony formation in soft agar.

Decreased cell adhesion, spreading, proliferation, migration and invasion in cells where RACK1 and PP2A binding is deficient suggests that the RACK1/PP2A complex has a role to play in maintaining the transformed phenotype in breast cancer. In order to investigate this hypothesis further, we determined whether disruption of the RACK1/PP2A complex had an effect on plating efficiency and/or the cells' ability to form colonies in soft agar. Results show that cells expressing a disruption to the RACK1/PP2A complex are deficient in plating efficiency (**Fig. 6a**). Data also shows that cells expressing a disruption to the RACK1/PP2A complex are deficient in the ability to form colonies in soft agar (**Fig. 6b**). This data supports our hypothesis that the interaction between RACK1 and PP2A helps to maintain the transformed phenotype in breast cancer cells.

4. Discussion

This study highlights that RACK1 stabilises PP2A activity and that the interaction between RACK1 and PP2A plays an essential role in cell adhesion, proliferation, migration and invasion of MCF-7 cells. PP2A is active when bound to RACK1 and we have demonstrated that reduced PP2A activity correlates with a reversal of the transformed phenotype. We have identified putative RACK1 interaction sites on the catalytic subunit of PP2A, and characterised a key role for the RACK1/PP2A complex in the progression and maintenance of the cancer phenotype. The first interaction locus we identified was FR69/70, and although surface exposed on the structure of RACK1, was found to have no effect on the binding of PP2A to RACK1. Although disruption at this site did alter PP2A activity levels in cells, the HA-PP2A FR69/70AA cell line showed no difference in the ability to adhere or invade. (**Supplementary Fig. 2**). The second RACK1 interaction site on PP2A that we identified encompassed Y218 and R214, residues proximal to the catalytic pocket of PP2A. Mutation of these two residues expressed in the context of full length RACK1 were deficient in RACK1 binding and also led to a decrease in PP2A activity, cell adhesion, cell proliferation, migration and invasion.

This work highlights a number of intriguing possibilities. It suggests that PP2A in complex with RACK1 may not be functioning as a tumour suppressor. Rather, we show that inhibition of PP2A activity through disruption of the RACK1/PP2A complex reduces cell adhesion, proliferation, migration and invasion. This strongly points towards PP2A having a pro-carcinogenic role to play in this cancer cell model when in complex with RACK1. RACK1 appears to have the ability to scaffold PP2A to sites and substrates involved in cancer progression, while, at the same time, RACK1 also plays an essential role in stabilizing PP2A phosphatase activity. Thus, the RACK1/PP2A complex may be considered as a potential therapeutic target for breast cancer in the future, and development of compounds

that disrupt the interaction between these two proteins might, in principle, serve to slow down the development and progression of a malignancy.

Inhibition of PP2A has already been the subject of many investigations as a therapeutic strategy in cancer in recent years (reviewed in [23]. Indeed, two PP2A-inhibitory compounds, LB-100 and LB-102 (from Lixte Biotechnology, Inc.), are now showing promise as chemotherapy drug sensitizers. LB-102 inhibits PP2A to increase the efficacy of drugs, including doxorubicin, in xenograph animal models of glioblastoma by blocking cellular DNA damage defence mechanisms that are targeted by the chemotherapeutic agent [37]. The related PP2A inhibitor, LB-100 (currently in clinical trials; NCT01837667 [56]), similarly enhances chemo-sensitivity to drugs in a number of cancer cell types, including sarcoma [57], pheochromocytoma [58], nasopharyngeal carcinoma [59], hepatocellular carcinoma [60], medulloblastoma [61] and pancreatic cancer [62, 63] as well as both breast [64] and ovarian cancers [65].

Given the broad substrate specificity and diverse cellular functions of PP2A, it is conceivable that selective disruption of RACK1-complexed pools of PP2A, as suggested by our model studies, might offer a more focused strategy for harnessing PP2A inhibition to treat cancer therapy, potentially decoupling pro-carcinogenic consequences of indiscriminate PP2A inhibition through PP2A-C site-directed competitive inhibitors. Interest in such finessed approaches to chemotherapeutic target exploitation is clearly increasing, as evinced by the growing body of work with IQ motif-containing GTPase activating protein 1 (IQGAP1) a scaffold within the MAPK pathway that is responsible for assembling the kinases within this pathway to effect signal transmission [66, 67]. IQGAP1 has been linked to the progression of cancer and drives tumourigenesis in both mouse models and human tissue [66, 68]. Up-regulation of the ERK1/2 MAPK cascade is seen in 30% of cancers and IQGAP1 binds to ERK1/2 through a highly conserved 32 amino acid ‘WW domain’ to

facilitate activation of ERK in response to certain stimuli. A specific YY/AA mutation in the IQGAP1 WW domain was found to disrupt the IQGAP1/ERK1/2 interaction, and this was sufficient to inhibit RAS driven-tumourigenesis, significantly increasing the life span of tumour bearing mice without having a negative effect on other proteins in the IQGAP1 interactome [66].

Deletion of RACK1 is embryonically lethal [69], whereas IQGAP1 knockout mice are viable [66], and clearly there may be challenges to achieving selective disruption of the RACK1-PP2A complex whilst avoiding interference with other RACK1 protein-protein interactions, at least in the case where a binding site on RACK1 is to be exploited. A key question, then, is whether it is feasible to block a scaffold protein such as RACK1 at a specific interaction point to gain a therapeutic benefit without disruption of its other functions. To date, no small molecule ligands for RACK1 have been reported, although foundational studies with peptidic ligands derived from RACK1 partner proteins have shown demonstrable potential as RACK1 complex disruptors in cell-based studies, notably in the case of the ternary FAK/RACK1/PDE4D5 ensemble that also plays a role in regulating cancer cell polarity, initiation of cancer cell spreading and metastasis [14, 15]. In this case, RACK1 binds to the FERM domain of FAK and serves to recruit PDE4D5, which in turn shapes cAMP gradients at nascent integrin adhesions. Disruption of the ternary complex by mutagenesis of two amino acids in the FAK FERM domain, so as to compromise the FAK-RACK1 interface, impaired cellular directional responses, and the same effect was achieved with a cell-permeabilised 38-mer peptide derived from the N-terminal region of PDE4D5 [70] that presumably binds to RACK1 and competitively blocks PDE4D5 recruitment. In this study by Serrels *et al* [14], disruption of the RACK1-PDE4D5 interaction with the peptide was achieved without evident disturbance to other vital RACK1 functions. Although small molecule ligands for RACK1 have yet to be identified, such compounds are beginning to

emerge for other RACK1-like β-propeller scaffolding proteins, with examples of both competitive and allosteric mechanisms of protein binding disruption [71-73]. Taken together with the work of Serrels *et al*, this suggests that selective disruption of RACK1 scaffolding interactions may be possible with small molecule ligands to provide a novel approach for therapeutic modulation of PP2A function whilst avoiding indiscriminate interference with other essential RACK1 functions.

Clearly, efforts to develop RACK1-PP2A disrupting agents would benefit from further definition of the nature of the RACK1-PP2A interaction, ideally with structural characterisation of the association. We have identified a candidate RACK1-binding surface on PP2A-C involving Y218 and possibly also the catalytic site residue, R214. Given the role of R214, it seems unlikely that RACK1 might bind to this residue whilst the enzyme is catalytically operational. However, at present we cannot exclude the possibility that RACK1 might have multiple roles in orchestrating PP2A function. For example, a direct interaction with R214 could conceivably invoke a 'transient' role in activating PP2A (*cf.* PTPA and LCMT-1, *vide supra*, **Section 3.1**), whilst Y218 might feature in a switched RACK1 association mode that serves to stabilise a particular PP2A holoenzyme assembly and/or target the complex to specific subcellular sites. The nature of the PP2A-binding site on RACK1 also requires clearer definition. Y302 in the WD-7 repeat of RACK1 has been implicated in the binding of both PP2A and β1 integrin [31]. Curiously Y302 is buried and does not exhibit surface exposure in the available RACK1 crystal structures. Any direct binding interaction involving Y302 would therefore require a conformational change in RACK1, and potentially involve propeller blade hairpin extrusion, as characterised [74] in the x-ray crystal structure of the yeast homologue (Asc1p) of RACK1 and postulated for other RACK1 protein associations [31]. Y302 is located on strand-B of propeller blade-7, as defined in [31], and might be exposed by extrusion of the outer C/D-strands in either blade-7

or blade-6, with the former linked to a conformationally mobile loop in the RACK1 structure. Such extrusion would expose a groove in the propeller rim as a potential protein binding site and might, in principle, be regulated by the phosphorylation status of the Y302.

In summary, in this study, we have further characterised the interaction between RACK1 and PP2A. Both proteins have a well-established relevance to breast cancer. We have determined that disruption of the RACK1/PP2A complex has implications for a wide range of cellular processes involved in maintenance and progression of cancer, including migration and invasion. Disruption of the RACK1/PP2A complex may have potential therapeutic benefit in breast cancer.

Acknowledgements

This work was supported by the Irish Cancer Society grant code CRS11KIE (MK), The Mid-Western Cancer Foundation (PK) and Science Foundation Ireland grant 13/CDA/2228 (PK). We also thank our colleagues in the Laboratory of Cellular and Molecular Biology for advice and critical analysis.

References

[1] D.R. Adams, D. Ron, P.A. Kiely, RACK1, A multifaceted scaffolding protein: Structure and function, Cell Communication and Signaling 9(1) (2011) 22.
[2] A. McCahill, J. Warwicker, G.B. Bolger, M.D. Houslay, S.J. Yarwood, The RACK1 scaffold protein: a dynamic cog in cell response mechanisms, Molecular Pharmacology 62(6) (2002) 1261-1273.
[3] D. Ron, D.R. Adams, G.S. Baillie, A. Long, R. O'Connor, P.A. Kiely, RACK (1) to the future-a historical perspective, Cell Communication and Signaling 11(1) (2013) 53.
[4] V. Gandin, D. Senft, I. Topisirovic, A.R. Ze'ev, RACK1 function in cell motility and protein synthesis, Genes & Cancer 4(9-10) (2013) 369-377.
[5] F. Battaini, A. Pascale, Protein kinase C signal transduction regulation in physiological and pathological aging, Annals of the New York Academy of Sciences 1057(1) (2005) 177-192.
[6] H.-Y. Wang, E. Friedman, Increased association of brain protein kinase C with the receptor for activated C kinase-1 (RACK1) in bipolar affective disorder, Biological Psychiatry 50(5) (2001) 364-370.
[7] Y. Ruan, L. Sun, Y. Hao, L. Wang, J. Xu, W. Zhang, J. Xie, L. Guo, L. Zhou, X. Yun, Ribosomal RACK1 promotes chemoresistance and growth in human hepatocellular carcinoma, The Journal of Clinical Investigation 122(122 (7)) (2012) 2554-2566.
[8] S.R. Williams, D.-S. Son, P.F. Terranova, Protein kinase C δ is activated in mouse ovarian surface epithelial cancer cells by 2, 3, 7, 8-tetrachlorodibenzo-p-dioxin (TCDD), Toxicology 195(1) (2004) 1-17.
[9] C.B. Hellberg, S.M. Burden-Gulley, G.E. Pietz, S.M. Brady-Kalnay, Expression of the receptor protein-tyrosine phosphatase, PTPμ, restores E-cadherin-dependent adhesion in human prostate carcinoma cells, Journal of Biological Chemistry 277(13) (2002) 11165-11173.
[10] X.X. Cao, J.D. Xu, X.L. Liu, J.W. Xu, W.J. Wang, Q.Q. Li, Q. Chen, Z.D. Xu, X.P. Liu, RACK1: A superior independent predictor for poor clinical outcome in breast cancer, International Journal of Cancer 127(5) (2010) 1172-1179.
[11] S. Al-Reefy, K. Mokbel, The role of RACK1 as an independent prognostic indicator in human breast cancer, Breast Cancer Research and Treatment 123(3) (2010) 911-912.
[12] P.A. Kiely, G.S. Baillie, R. Barrett, D.A. Buckley, D.R. Adams, M.D. Houslay, R. O'Connor, Phosphorylation of RACK1 on tyrosine 52 by c-Abl is required for insulin-like growth factor I-mediated regulation of focal adhesion kinase, Journal of Biological Chemistry 284(30) (2009) 20263-20274.
[13] S. Dwane, E. Durack, R. O'Connor, P.A. Kiely, RACK1 promotes neurite outgrowth by scaffolding AGAP2 to FAK, Cellular Signalling 26(1) (2014) 9-18.
[14] B. Serrels, E. Sandilands, A. Serrels, G. Baillie, M.D. Houslay, V.G. Brunton, M. Canel, L.M. Machesky, K.I. Anderson, M.C. Frame, A complex between FAK, RACK1, and PDE4D5 controls spreading initiation and cancer cell polarity, Current Biology 20(12) (2010) 1086-1092.
[15] B. Serrels, E. Sandilands, M.C. Frame, Signaling of the direction-sensing FAK/RACK1/PDE4D5 complex to the small GTPase Rap1, Small GTPases 2(1) (2011) 54-61.
[16] J. Li, Y. Guo, X. Feng, Z. Wang, Y. Wang, P. Deng, D. Zhang, R. Wang, L. Xie, X. Xu, Receptor for activated C kinase 1 (RACK1): a regulator for migration and invasion in oral squamous cell carcinoma cells, Journal of Cancer Research and Clinical Oncology 138(4) (2012) 563-571.
[17] S. Shi, Y.-Z. Deng, J.-S. Zhao, X.-D. Ji, J. Shi, Y.-X. Feng, G. Li, J.-J. Li, D. Zhu, H.P. Koeffler, RACK1 promotes non-small-cell lung cancer tumorigenicity through activating sonic hedgehog signaling pathway, Journal of Biological Chemistry 287(11) (2012) 7845-7858.
[18] Z. Wang, B. Zhang, L. Jiang, X. Zeng, Y. Chen, X. Feng, Y. Guo, Q. Chen, RACK1, an excellent predictor for poor clinical outcome in oral squamous carcinoma, similar to Ki67, European Journal of Cancer 45(3) (2009) 490-496.
[19] X.-X. Cao, J.-D. Xu, J.-W. Xu, X.-L. Liu, Y.-Y. Cheng, W.-J. Wang, Q.-Q. Li, Q. Chen, Z.-D. Xu, X.-P. Liu, RACK1 promotes breast carcinoma proliferation and invasion/metastasis in vitro and in vivo, Breast Cancer Research and Treatment 123(2) (2010) 375-386.
[20] J. Li, D. Xie, RACK1, a versatile hub in cancer, Oncogene (2014).

[21] B.A. Hemmings, C. Adams-Pearson, F. Maurer, P. Mueller, J. Goris, W. Merlevede, J. Hofsteenge, S.R. Stone, . alpha.-And. beta.-forms of the 65-kDa subunit of protein phosphatase 2A have a similar 39 amino acid repeating structure, Biochemistry 29(13) (1990) 3166-3173.
[22] S.R. Stone, J. Hofsteenge, B.A. Hemmings, Molecular cloning of cDNAs encoding two isoforms of the catalytic subunit of protein phosphatase 2A, Biochemistry 26(23) (1987) 7215-7220.
[23] M. Kiely, P.A. Kiely, PP2A: The Wolf in Sheep's Clothing?, Cancers 7(2) (2015) 648-669.
[24] P. Seshacharyulu, P. Pandey, K. Datta, S.K. Batra, Phosphatase: PP2A structural importance, regulation and its aberrant expression in cancer, Cancer Letters 335(1) (2013) 9-18.
[25] V. Janssens, J. Goris, Protein phosphatase 2A: a highly regulated family of serine/threonine phosphatases implicated in cell growth and signalling, Biochem. J 353 (2001) 417-439.
[26] A.H. Schönthal, Role of serine/threonine protein phosphatase 2A in cancer, Cancer Letters 170(1) (2001) 1-13.
[27] D. Perrotti, P. Neviani, Protein phosphatase 2A: a target for anticancer therapy, The Lancet Oncology 14(6) (2013) e229-e238.
[28] S. Ugi, T. Imamura, W. Ricketts, J.M. Olefsky, Protein phosphatase 2A forms a molecular complex with Shc and regulates Shc tyrosine phosphorylation and downstream mitogenic signaling, Molecular and Cellular Biology 22(7) (2002) 2375-2387.
[29] S. Ugi, T. Imamura, H. Maegawa, K. Egawa, T. Yoshizaki, K. Shi, T. Obata, Y. Ebina, A. Kashiwagi, J.M. Olefsky, Protein phosphatase 2A negatively regulates insulin's metabolic signaling pathway by inhibiting Akt (protein kinase B) activity in 3T3-L1 adipocytes, Molecular and Cellular Biology 24(19) (2004) 8778-8789.
[30] P.A. Kiely, D. O'Gorman, K. Luong, D. Ron, R. O'Connor, Insulin-like growth factor I controls a mutually exclusive association of RACK1 with protein phosphatase 2A and β1 integrin to promote cell migration, Molecular and Cellular Biology 26(11) (2006) 4041-4051.
[31] P.A. Kiely, G.S. Baillie, M.J. Lynch, M.D. Houslay, R. O'Connor, Tyrosine 302 in RACK1 is essential for insulin-like growth factor-I-mediated competitive binding of PP2A and β1 integrin and for tumor cell proliferation and migration, Journal of Biological Chemistry 283(34) (2008) 22952-22961.
[32] A. Kurimchak, X. Graña, PP2A holoenzymes negatively and positively regulate cell cycle progression by dephosphorylating pocket proteins and multiple CDK substrates, Gene 499(1) (2012) 1-7.
[33] I.-M. Shih, P.K. Panuganti, K.-T. Kuo, T.-L. Mao, E. Kuhn, S. Jones, V.E. Velculescu, R.J. Kurman, T.-L. Wang, Somatic Mutations of< i> PPP2R1A</i> in Ovarian and Uterine Carcinomas, The American Journal of Pathology 178(4) (2011) 1442-1447.
[34] R. Ruediger, H.T. Pham, G. Walter, Disruption of protein phosphatase 2A subunit interaction in human cancers with mutations in the Aα subunit gene, Oncogene 20(1) (2001).
[35] W. Li, L. Xie, Z. Chen, Y. Zhu, Y. Sun, Y. Miao, Z. Xu, X. Han, Cantharidin, a potent and selective PP2A inhibitor, induces an oxidative stress‐independent growth inhibition of pancreatic cancer cells through G2/M cell‐cycle arrest and apoptosis, Cancer Science 101(5) (2010) 1226-1233.
[36] F.H. Duong, M.T. Dill, M.S. Matter, Z. Makowska, D. Calabrese, T. Dietsche, S. Ketterer, L. Terracciano, M.H. Heim, Protein phosphatase 2A promotes hepatocellular carcinogenesis in the diethylnitrosamine mouse model through inhibition of p53, Carcinogenesis 35(1) (2014) 114-122.
[37] J. Lu, J.S. Kovach, F. Johnson, J. Chiang, R. Hodes, R. Lonser, Z. Zhuang, Inhibition of serine/threonine phosphatase PP2A enhances cancer chemotherapy by blocking DNA damage induced defense mechanisms, Proceedings of the National Academy of Sciences 106(28) (2009) 11697-11702.
[38] R. Boudreau, D.M. Conrad, D.W. Hoskin, Apoptosis induced by protein phosphatase 2A (PP2A) inhibition in T leukemia cells is negatively regulated by PP2A-associated p38 mitogen-activated protein kinase, Cellular Signalling 19(1) (2007) 139-151.
[39] C.S. Hong, M.J. Feldman, Z. Zhuang, Targeting protein phosphatase 2A to overcome tumor senescence in gynecologic and breast cancers, American Journal of Clinical and Experimental Obstetrics and Gynecology 2(3) (2015) 144-150.

[40] R. Frank, The SPOT-synthesis technique. Synthetic peptide arrays on membrane supports--principles and applications, J Immunol Methods 267(1) (2002) 13-26.
[41] R. Frank, H. Overwin, SPOT synthesis. Epitope analysis with arrays of synthetic peptides prepared on cellulose membranes, Methods Mol Biol 66 (1996) 149-69.
[42] A. Kramer, J. Schneider-Mergener, Synthesis and screening of peptide libraries on continuous cellulose membrane supports, Combinatorial Peptide Library Protocols, Springer1998, pp. 25-39.
[43] S. Dwane, P.A. Kiely, Tools used to study how protein complexes are assembled in signaling cascades, Bioengineered Bugs 2(5) (2011) 247-259.
[44] Y. Xu, Y. Xing, Y. Chen, Y. Chao, Z. Lin, E. Fan, J. Yu, W,, S. Strack, P.D. Jeffrey, Y. Shi, Structure of the Protein Phosphatase 2A Holoenzyme, Cell 127(6) (2006) 1239-1251.
[45] U.S. Cho, W. Xu, Crystal structure of a protein phosphatase 2A heterotrimeric holoenzyme, Nature 445(7123) (2007) 53-57.
[46] Y. Xu, Y. Chen, P. Zhang, P.D. Jeffrey, Y. Shi, Structure of a Protein Phosphatase 2A Holoenzyme: Insights into B55-Mediated Tau Dephosphorylation, Molecular Cell 31(6) (2008) 873-885.
[47] Z. Xu, B. Cetin, M. Anger, U.S. Cho, W. Helmhart, K. Nasmyth, W. Xu, Structure and function of the PP2A-shugoshin interaction, Molecular Cell 35(4) (2009) 426-441.
[48] N. Wlodarchak, F. Guo, K.A. Satyshur, L. Jiang, P.D. Jeffrey, T. Sun, V. Stanevich, M.C. Mumby, Y. Xing, Structure of the Ca2+-dependent PP2A heterotrimer and insights into Cdc6 dephosphorylation, Cell Research 23(7) (2013) 931-946.
[49] Y. Xing, Y. Xu, Y. Chen, P.D. Jeffrey, Y. Chao, Z. Lin, Z. Li, S. Strack, J.B. Stock, Y. Shi, Structure of protein phosphatase 2A core enzyme bound to tumor-inducing toxins, Cell 127(2) (2006) 341-353.
[50] H. Hombauer, D. Weismann, I. Mudrak, C. Stanzel, T. Fellner, D.H. Lackner, E. Ogris, Generation of active protein phosphatase 2A is coupled to holoenzyme assembly, PLoS Biology 5(6) (2007) e155.
[51] F. Guo, V. Stanevich, N. Wlodarchak, R. Sengupta, L. Jiang, K.A. Satyshur, Y. Xing, Structural basis of PP2A activation by PTPA, an ATP-dependent activation chaperone, Cell Research 24(2) (2014) 190-203.
[52] J. Lee, J. Stock, Protein phosphatase 2A catalytic subunit is methyl-esterified at its carboxyl terminus by a novel methyltransferase, Journal of Biological Chemistry 268(26) (1993) 19192-19195.
[53] I. De Baere, R. Derua, V. Janssens, C. Van Hoof, E. Waelkens, W. Merlevede, J. Goris, Purification of porcine brain protein phosphatase 2A leucine carboxyl methyltransferase and cloning of the human homologue, Biochemistry 38(50) (1999) 16539-16547.
[54] V. Stanevich, L. Jiang, K.A. Satyshur, Y. Li, P.D. Jeffrey, Z. Li, P. Menden, M.F. Semmelhack, Y. Xing, The structural basis for tight control of PP2A methylation and function by LCMT-1, Molecular Cell 41(3) (2011) 331-342.
[55] T.S. Kitajima, Sakuno, T., Ishiguro, K., Lemura, S., Natsume, T., Kawashima, S. A., Watanabe, Y., Shugoshin collaborates with protein phosphatase 2A to protect cohesin., Nature 441 (2006) 46-52.
[56] V. Chung, A. Mansfield, J. Kovach, A phase 1 study of a novel inhibitor of protein phosphatase 2A alone and with docetaxel, Journal of Clinical Oncology 32(5s) (2014) TS2636.
[57] C. Zhang, C.S. Hong, X. Hu, C. Yang, H. Wang, D. Zhu, S. Moon, P. Dmitriev, J. Lu, J. Chiang, Inhibition of protein phosphatase 2A with the small molecule LB100 overcomes cell cycle arrest in osteosarcoma after cisplatin treatment, Cell Cycle (just-accepted) (2015) 00-00.
[58] L. Martiniova, J. Lu, J. Chiang, M. Bernardo, R. Lonser, Z. Zhuang, K. Pacak, Pharmacologic modulation of serine/threonine phosphorylation highly sensitizes PHEO in a MPC cell and mouse model to conventional chemotherapy, PloS one 6(2) (2011) e14678.
[59] P. Lv, Y. Wang, J. Ma, Z. Wang, J.-L. Li, C.S. Hong, Z. Zhuang, Y.-X. Zeng, Inhibition of protein phosphatase 2A with a small molecule LB100 radiosensitizes nasopharyngeal carcinoma xenografts by inducing mitotic catastrophe and blocking DNA damage repair, Oncotarget 5(17) (2014) 7512.
[60] X.-L. Bai, Q. Zhang, L.-Y. Ye, Q.-D. Hu, Q.-H. Fu, X. Zhi, W. Su, R.-G. Su, T. Ma, W. Chen, Inhibition of protein phosphatase 2A enhances cytotoxicity and accessibility of chemotherapeutic drugs to hepatocellular carcinomas, Molecular Cancer Therapeutics 13(8) (2014) 2062-2072.

[61] W. Ho, M. Feldman, D. Maric, L. Amable, M. Hall, G. Feldman, A. Ray-Chaudhury, M. Lizak, J. Vera, R. Robison, PP2A inhibition with LB100 enhances cisplatin cytotoxicity and overcomes cisplatin resistance in medulloblastoma cells, Oncotarget (2016).
[62] D. Wei, L.A. Parsels, D. Karnak, M.A. Davis, J.D. Parsels, A.C. Marsh, L. Zhao, J. Maybaum, T.S. Lawrence, Y. Sun, Inhibition of protein phosphatase 2A radiosensitizes pancreatic cancers by modulating CDC25C/CDK1 and homologous recombination repair, Clinical Cancer Research 19(16) (2013) 4422-4432.
[63] X. Bai, X. Zhi, Q. Zhang, F. Liang, W. Chen, C. Liang, Q. Hu, X. Sun, Z. Zhuang, T. Liang, Inhibition of protein phosphatase 2A sensitizes pancreatic cancer to chemotherapy by increasing drug perfusion via HIF-1α-VEGF mediated angiogenesis, Cancer Letters 355(2) (2014) 281-287.
[64] J. Xu, Z. Xu, J.-Y. Zhou, Z. Zhuang, E. Wang, J. Boerner, G.S. Wu, Regulation of the Src-PP2A interaction in tumor necrosis factor (TNF)-related apoptosis-inducing ligand (TRAIL)-induced apoptosis, Journal of Biological Chemistry 288(46) (2013) 33263-33271.
[65] K.-E. Chang, B.-R. Wei, J.P. Madigan, M.D. Hall, R.M. Simpson, Z. Zhuang, M.M. Gottesman, The protein phosphatase 2A inhibitor LB100 sensitizes ovarian carcinoma cells to cisplatin-mediated cytotoxicity, Molecular Cancer Therapeutics 14(1) (2015) 90-100.
[66] K.L. Jameson, P.K. Mazur, A.M. Zehnder, J. Zhang, B. Zarnegar, J. Sage, P.A. Khavari, IQGAP1 scaffold-kinase interaction blockade selectively targets RAS-MAP kinase-driven tumors, Nature Medicine 19(5) (2013) 626-630.
[67] Z. Li, S.H. Kim, J.M. Higgins, M.B. Brenner, D.B. Sacks, IQGAP1 and calmodulin modulate E-cadherin function, Journal of Biological Chemistry 274(53) (1999) 37885-37892.
[68] L. Jadeski, J.M. Mataraza, H.-W. Jeong, Z. Li, D.B. Sacks, IQGAP1 stimulates proliferation and enhances tumorigenesis of human breast epithelial cells, Journal of Biological Chemistry 283(2) (2008) 1008-1017.
[69] V. Volta, A. Beugnet, S. Gallo, L. Magri, D. Brina, E. Pesce, P. Calamita, F. Sanvito, S. Biffo, RACK1 depletion in a mouse model causes lethality, pigmentation deficits and reduction in protein synthesis efficiency, Cellular and Molecular Life Sciences 70(8) (2013) 1439-1450.
[70] K.J. Smith, G.S. Baillie, E.I. Hyde, X. Li, T.M. Houslay, A. McCahill, A.J. Dunlop, G.B. Bolger, E. Klussmann, D.R. Adams, 1 H NMR structural and functional characterisation of a cAMP-specific phosphodiesterase-4D5 (PDE4D5) N-terminal region peptide that disrupts PDE4D5 interaction with the signalling scaffold proteins, βarrestin and RACK1, Cellular Signalling 19(12) (2007) 2612-2624.
[71] S. Guillermo, W. Hong, A.-H. Abdellah, A.W. Gregory, B.-L. Dalia, D. Ludmila, D. Aiping, T.N. Kong, S. David, B. Yuri, Small-molecule inhibition of MLL activity by disruption of its interaction with WDR5, Biochemical Journal 449(1) (2013) 151-159.
[72] H. Karatas, E.C. Townsend, F. Cao, Y. Chen, D. Bernard, L. Liu, M. Lei, Y. Dou, S. Wang, High-affinity, small-molecule peptidomimetic inhibitors of MLL1/WDR5 protein–protein interaction, Journal of the American Chemical Society 135(2) (2012) 669-682.
[73] S. Orlicky, X. Tang, V. Neduva, N. Elowe, E.D. Brown, F. Sicheri, M. Tyers, An allosteric inhibitor of substrate recognition by the SCFCdc4 ubiquitin ligase, Nature Biotechnology 28(7) (2010) 733-737.
[74] L. Yatime, K.L. Hein, J. Nilsson, P. Nissen, Structure of the RACK1 dimer from Saccharomyces cerevisiae, Journal of Molecular Biology 411(2) (2011) 486-498.

Figure Legends.

Figure 1. Mapping the interaction between RACK1 and the PP2A-C subunit. (a)(i) HA-tagged Empty Vector and PP2A WT were transfected into MCF-7 cells. The cells were lysed and a RACK1 IP was performed and analysed for associated HA-PP2A-C by western blotting using a HA antibody. Panel on the right shows the corresponding cell lysates. **(ii)** MCF-7 cells were lysed and a PP2A-C IP was performed and analysed for associated RACK1 by western blotting. n=3. **(b)** Peptide arrays encompassing the entire PP2A-C subunit were generated. Arrays were probed with GST-RACK1, which was detected by immunoblotting with anti-GST antibody. Two arrays gave a similar pattern of RACK1 binding. Array shown is representative of the two independent arrays. Positively interacting peptides generated dark spots and non-interacting peptides left blank spots. The array control conditions used GST alone as the probe. After immunoblotting with anti-GST antibody, we considered peptides to be positive when the interaction was distinctly higher that any spots when probed with GST alone (n=3).

Figure 2. Candidate RACK1 binding site analysis and disrupting the RACK1/PP2A interaction decreases the phosphatase activity of PP2A. (a) Interaction-positive sequences identified in Figure 1(b) were further analysed using alanine substitution. Alanine-scanning progeny arrays were generated by successive substitution of individual residues in the parent peptide array sequences with alanine (or aspartic acid for alanine). The progeny arrays (in 18-mer format) were probed with GST-RACK1 as per Figure 1(b). Representative results are shown for progeny arrays derived from parent peptides A14 and C12. The alanine-substituted residues in progeny peptides with reduced GST-RACK1 binding relative to wild-type sequence control peptide (Co) are potentially implicated in RACK1 binding. Attention was focused on residues whose substitution by alanine afforded an average of 50% less binding over the three experiments. In each case the array shown is representative of one of three 18-mer alanine scanning progeny arrays analysed for the regions encompassing parent peptides A12-A15 and C9-C13, with F69, R70, R214 and Y218 consistently implicated as key residues for RACK1 interaction. **(b)** Inspection of the available PP2A crystal structures confirmed the accessibility of residues (F69, R70, R214, Y218) identified from the progeny peptide arrays as candidate RACK1 interaction points. The surface-exposed locations of F69/R70 **(i)** and R214/Y218 **(ii)** are shown, here mapped onto the PP2A ternary holoenzyme co-crystal structure (PDB: 3DW8) with microcystin-LR. R214 plays a key role in substrate binding and maintenance of the active site region architecture as shown in (iii) **(c)** HA-tagged PP2A mutants were transfected into MCF-7 cells and stable cell lines were selected using G418. A RACK1 IP was performed on the HA-tagged PP2A stable mutant cell lines and analysed for associated HA by western blotting. Lysates were analysed for associated HA and actin by Western blotting n=3 **(d)** Cellular PP2A activity was measured using a PP2A immunoprecipitation phosphatase assay kit. MCF-7 cells expressing HA-PP2A WT, HA-PP2A FR69/70AA, HA-PP2A R214A and HA-PP2A Y218F were immunoprecipitated using an anti-HA antibody and the samples were analysed in a colorimetric assay at 650 nm. PP2A activity levels of MCF-7 cells expressing HA-PP2A FR69/70AA, HA-PP2A R214A and HA-PP2A Y218F were compared to activity levels of HA-PP2A WT. *$p<0.01$ (n=3).

Figure 3. The RACK1/PP2A complex is required for cell adhesion and spreading. Cellular spreading was monitored using the xCELLigence system. **(a)** The xCELLigence graph is representative of the average of duplicate wells from one experiment comparing cellular spreading of PP2A mutant stable cell lines HA-PP2A WT cells to the cellular spreading of HA-PP2A R214A and HA-PP2A Y218F cells. Bar graph shows difference in cell index between the cellular spreading of HA-PP2A WT (control) cells and both HA-PP2A R214A and HA-PP2A Y218F cells. Readings expressed as CI values. **(b)** 2,000 cells of the PP2A mutant stable cell lines HA-PP2A WT, HA-PP2A R214A and HA-PP2A Y218F were plated in collagen coated wells, incubated for one hour, washed, fixed in 100µl methanol and stained with 0.1% crystal violet. Cells were washed again and Triton X was added to the wells. After drying, the plates were read at 590 nm. Adhesion of HA-PP2A R214A and HA-PP2A Y218F cells were compared to adhesion of HA-PP2A WT. *$p<0.05$, **$p<0.01$, ***$p<0.001$. n=3.

Figure 4. Disruption of the RACK1/PP2A complex decreases cellular proliferation and migration. Proliferation was monitored in real time using the xCELLigence system. Readings expressed as CI values. **(a) (i)** The xCELLigence graph is the average of duplicate wells comparing proliferation of PP2A mutant stable cell lines HA-PP2A WT cells compared to HA-PP2A R214A cells and HA-PP2A Y218F cells over 48 hours. **(ii)** Bar graph comparing the mean CI over 12, 24 and 48 hours. **(iii)** Bar graph representing a comparison of the percentage difference in mean cell index of PP2A mutant stable cell line HA-PP2A WT with HA-PP2A R214A and HA-PP2A Y218F cells at 48 hours. *$p<0.05$, ***$p<0.001$ compared to the WT control. n=3. **(b)** Migration of the stable PP2A mutants compared to the wild type control. Percentage wound closure of HA-PP2A WT was compared to the percentage wound closure of HA-PP2A R214A and HA-PP2A Y218F after 24 hours.

Figure 5. Disruption of the RACK1/PP2A complex decreases cellular invasion. Cell invasion of PP2A mutant stable cell lines HA-PP2A WT, HA-PP2A R214A and HA-PP2A Y218F was monitored in real-time with xCELLigence system CIM-plates. **(a)(i)** Representative xCELLigence graph **(ii)** Invasion of HA-PP2A WT compared to HA-PP2A R214A and HA-PP2A Y218F was compared over 24, 36, 48, 60 and 72 hours. ***$p<0.001$ compared to the WT control. **(iii)** Percentage difference in cell index of HA-PP2A WT compared to HA-PP2A R214A and HA-PP2A Y218F at 72 hours (n=3).

Figure 6. The RACK1/PP2A complex is required for the maintenance of the transformed phenotype. (a) Plating efficiency assay showing difference in colony number between HA-PP2A WT, HA-PP2A R214A and HA-PP2A Y218F. **(b)** Cell were grown in soft agar, counted and compared against the wild type control.

Supplementary Figure 1.

HEK cells were transiently transfected with the HA-tagged PP2A mutants, HA-PP2A WT, HA-PP2A R214A and HA-PP2A Y218F. A RACK1 IP was performed and analysed for associated HA by western blotting.

Supplementary Figure 2.

Mutating the PP2A-C subunit at site F69/R70 has no effect on cellular adhesion or invasion.

2,000 cells of the PP2A mutant stable cell lines HA-PP2A WT and HA-PP2A FR69/70AA were plated in collagen coated wells, incubated for one hour, washed, fixed in 100µl methanol and stained with 0.1% crystal violet. Cells were washed again and Triton X was added to the wells. After drying, the plates were read at 590 nm. Adhesion of HA-PP2A FR69/70AA cells were compared to adhesion of HA-PP2A WT. Cell invasion of PP2A mutant stable cell lines HA-PP2A WT and HA-PP2A FR69/70AA was monitored in real-time with xCELLigence system CIM-plates. **(d)(i)** Representative xCELLigence graph **(ii)** Invasion of HA-PP2A WT compared to HA-PP2A FR69/70AA was compared over 72 hours.

Figure 1

(a) (i)

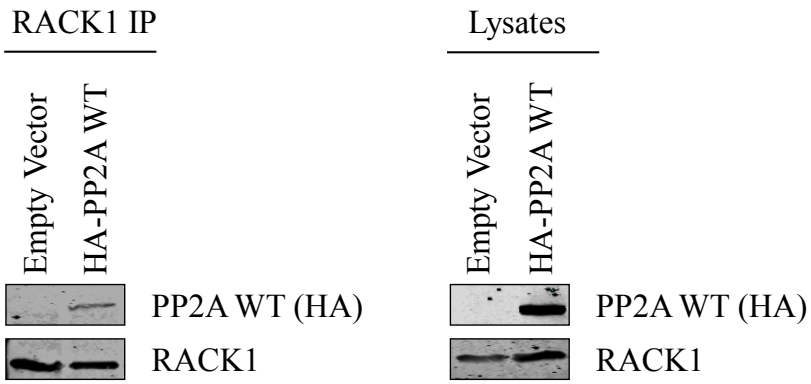

(ii)

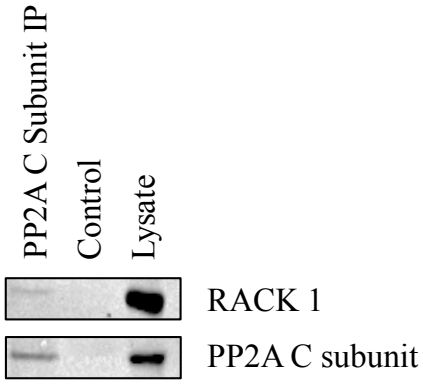

(b)

Array: PP2A (A) catalytic subunit

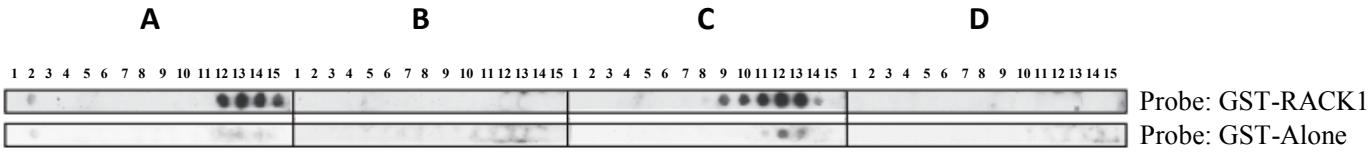

23-mer peptide sequence	Residues	Peptide Spot
GDVHGQFHDLMELFRIGGKSPDT	56-78	A12
QFHDLMELFRIGGKSPDTNYLFM	61-83	A13
MELFRIGGKSPDTNYLFMGDYVD	66-88	A14
IGGKSPDTNYLFMGDYVDRGYYS	71-93	A15
HEGPMCDLLWSDPDDRGGWGISP	191-213	C9
CDLLWSDPDDRGGWGISPRGAGY	196-218	C10
SDPDDRGGWGISPRGAGYTFGQD	201-223	C11
RGGWGISPRGAGYTFGQDISETF	206-228	C12
ISPRGAGYTFGQDISETFNHANG	211-233	C13

Figure 2

(a)

Array: PP2A (A) catalytic subunit

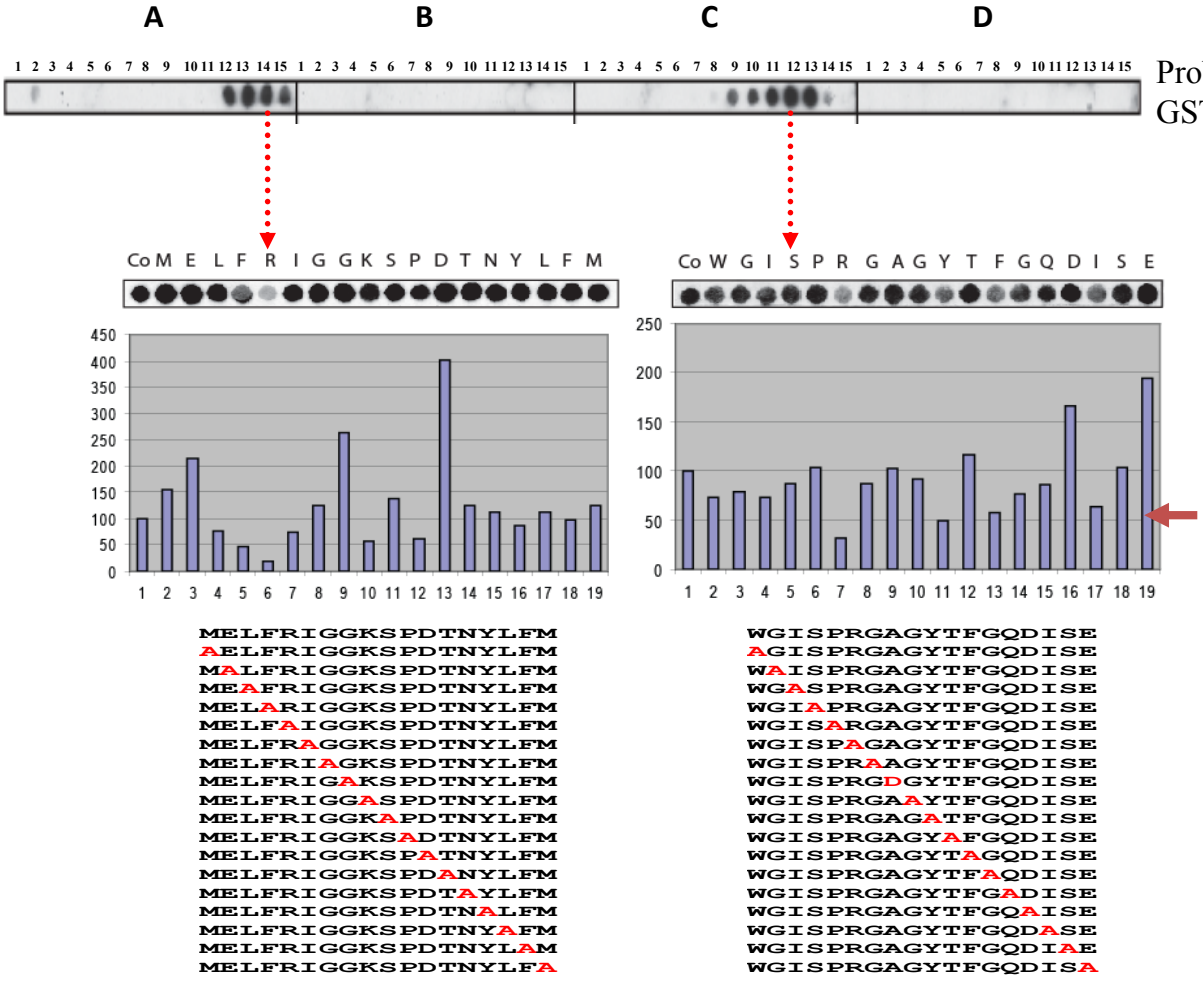

(b)(i)

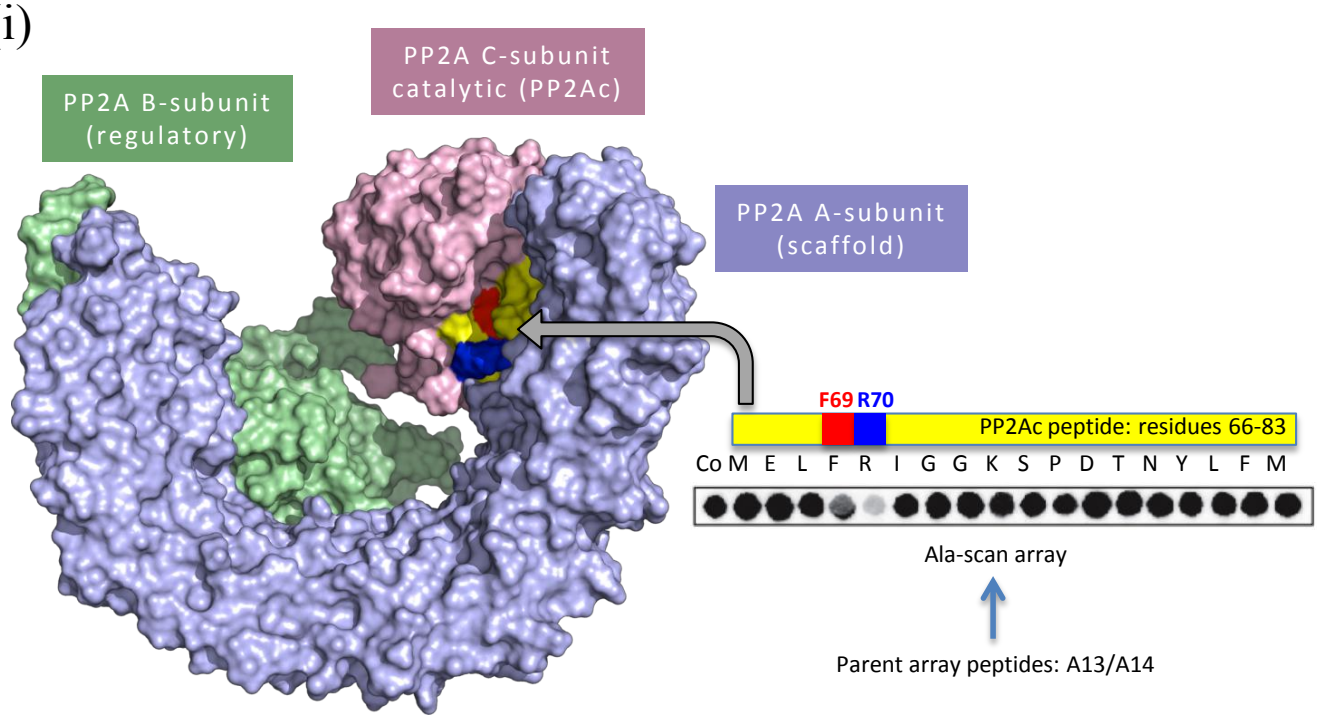
PP2A B-subunit (regulatory)
PP2A C-subunit catalytic (PP2Ac)
PP2A A-subunit (scaffold)
F69 R70
PP2Ac peptide: residues 66-83
Co M E L F R I G G K S P D T N Y L F M
Ala-scan array
Parent array peptides: A13/A14

(ii)

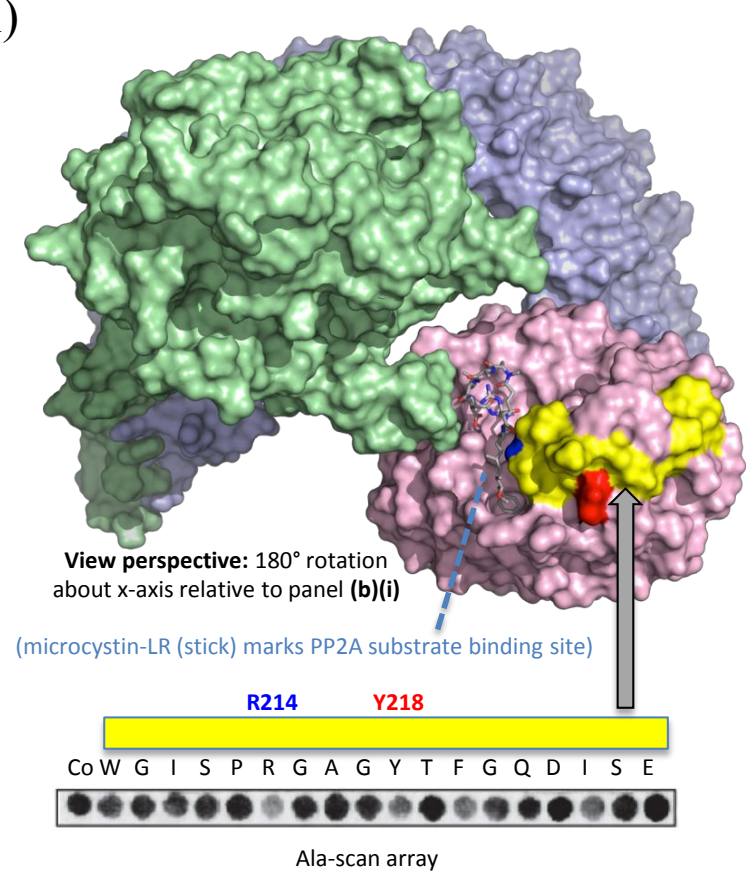
View perspective: 180° rotation about x-axis relative to panel (b)(i)
(microcystin-LR (stick) marks PP2A substrate binding site)
R214
Y218
Co W G I S P R G A G Y T F G Q D I S E
Ala-scan array

(iii)

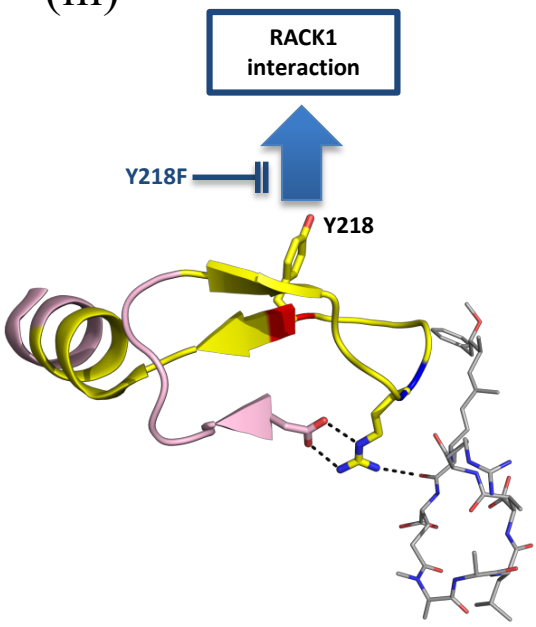
RACK1 interaction
Y218F
Y218

(c)

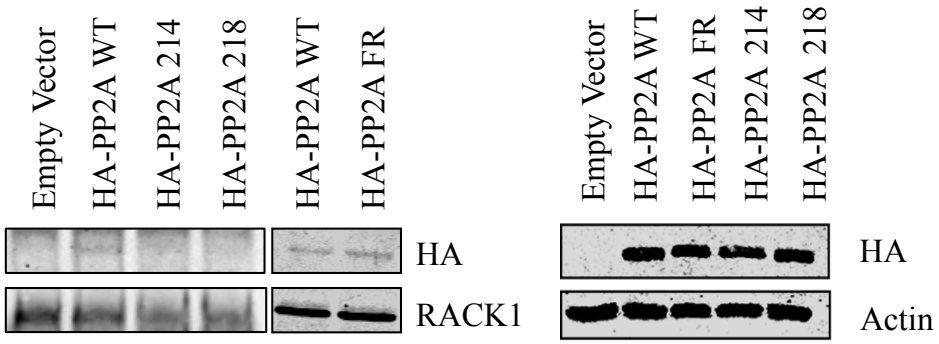
Empty Vector
HA-PP2A WT
HA-PP2A 214
HA-PP2A 218
HA-PP2A WT
HA-PP2A FR
HA
RACK1
Empty Vector
HA-PP2A WT
HA-PP2A FR
HA-PP2A 214
HA-PP2A 218
HA
Actin

(d)

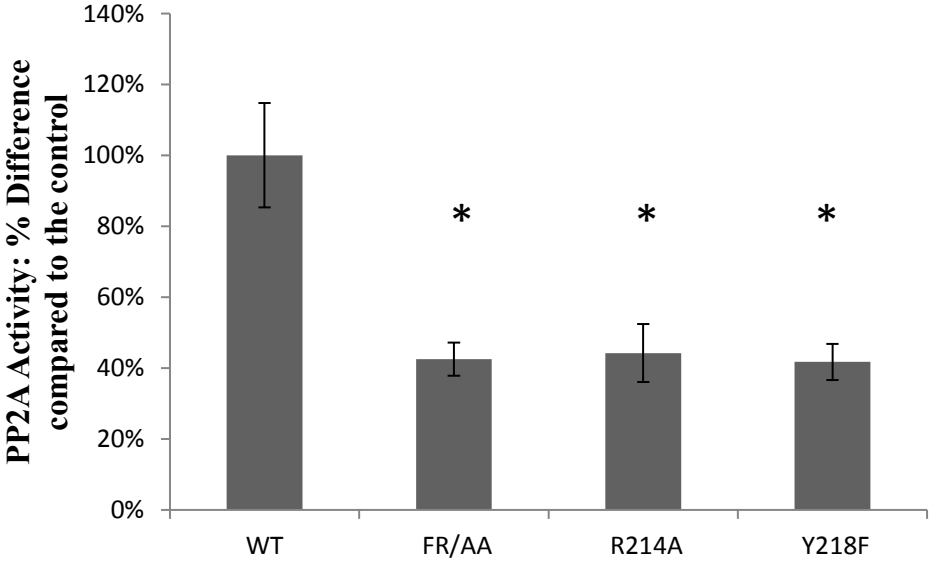
PP2A Activity: % Difference compared to the control
140%
120%
100%
80%
60%
40%
20%
0%
*
*
*
WT
FR/AA
R214A
Y218F

Figure 3

(a) (i)

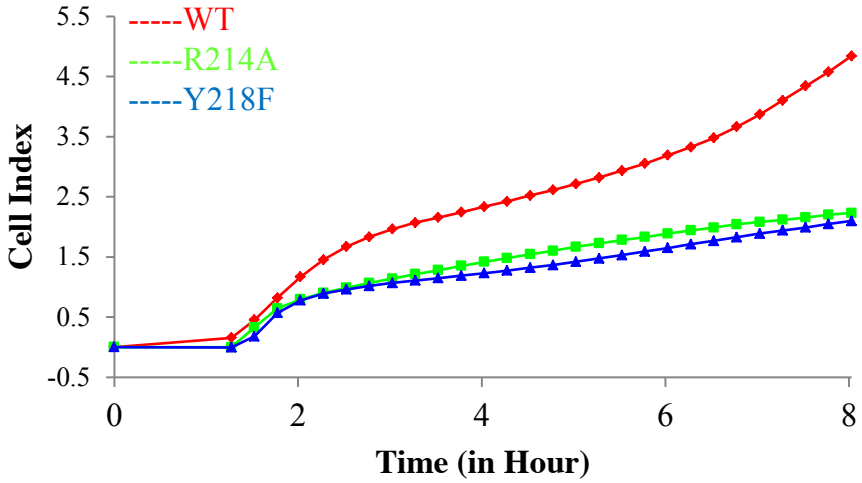

(ii)

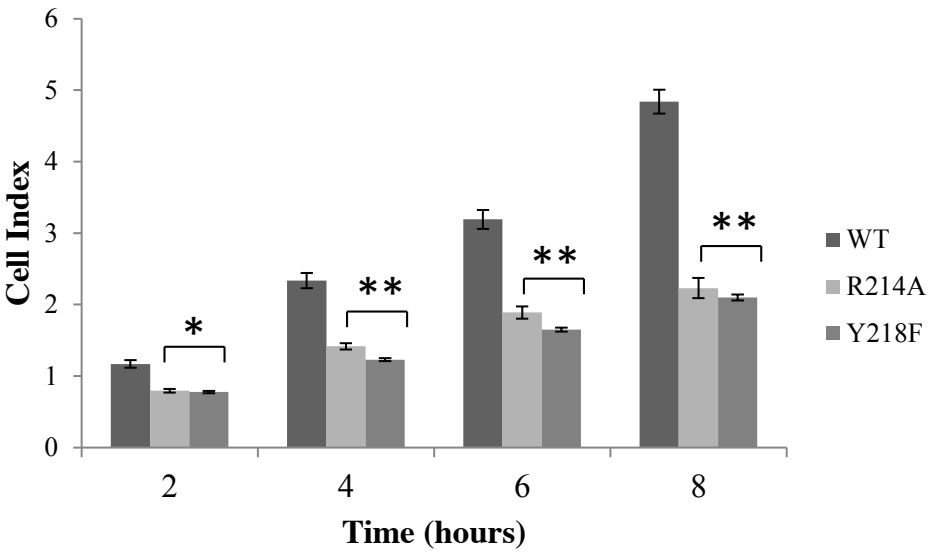

(b)

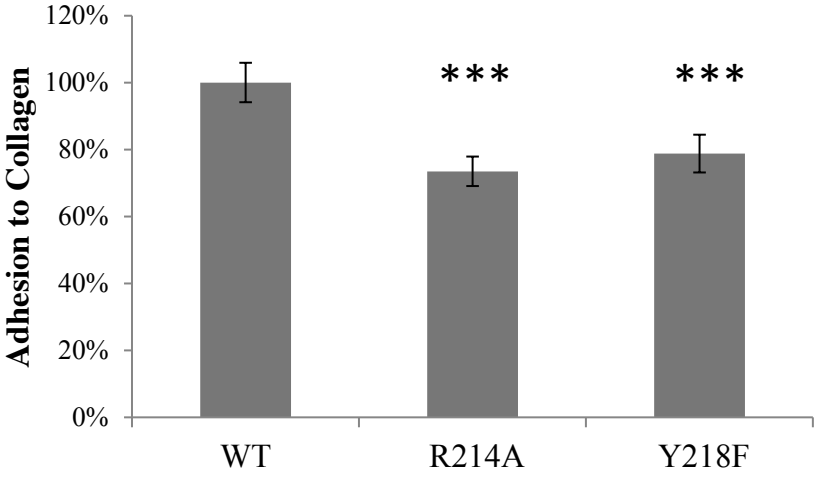

Figure 4

(a)(i)

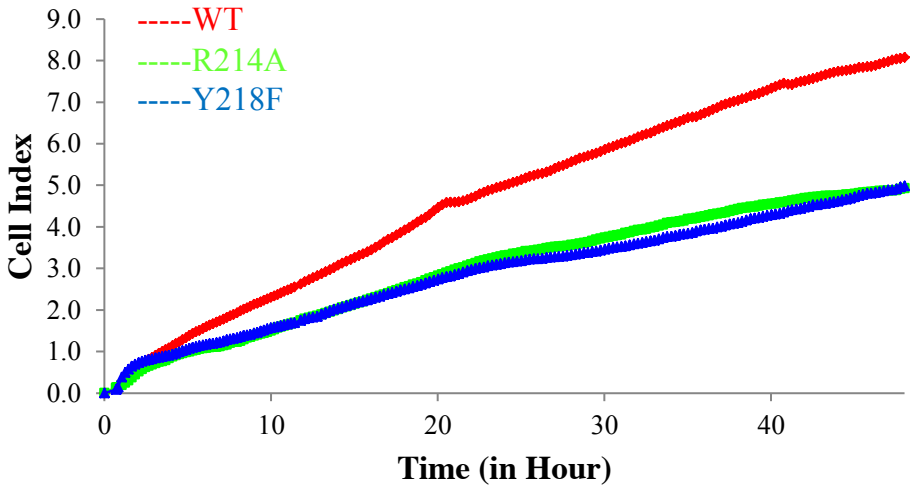

(ii)

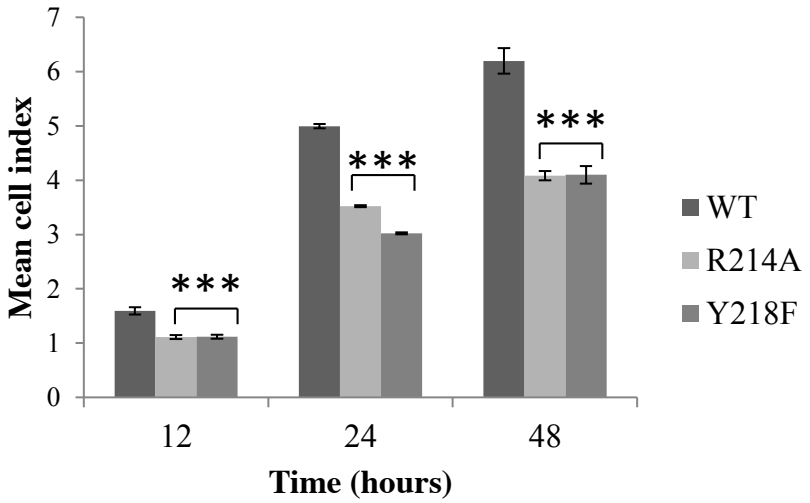

(iii)

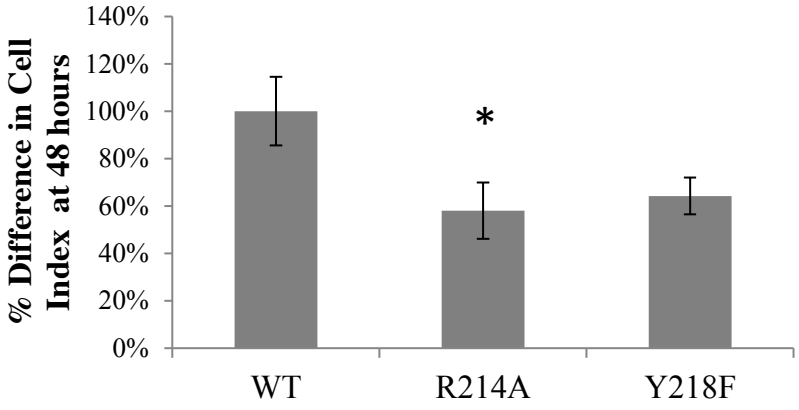

(b)

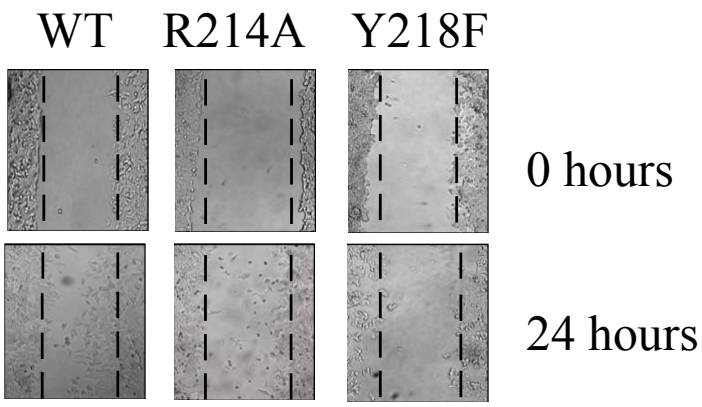
WT
R214A
Y218F
0 hours
24 hours

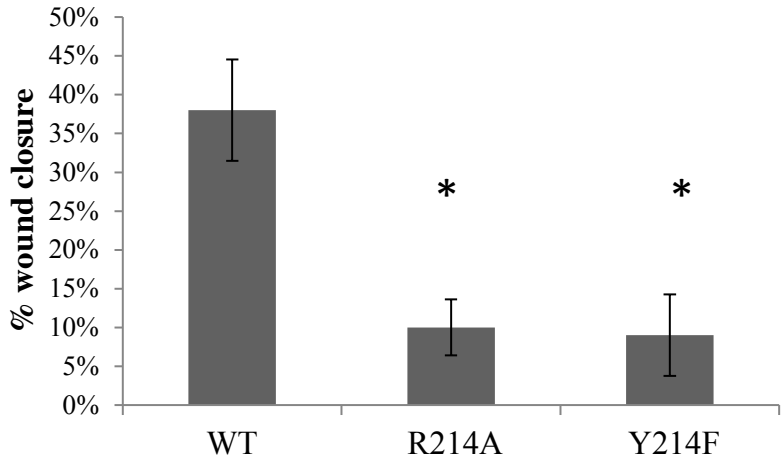
% wound closure
50%
45%
40%
35%
30%
25%
20%
15%
10%
5%
0%
*
*
WT
R214A
Y214F

Figure 5

(a)(i)

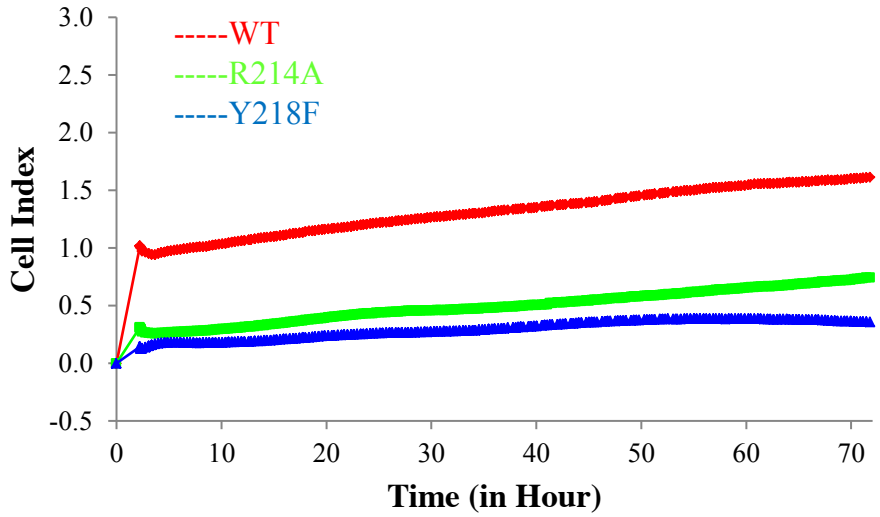

(ii)

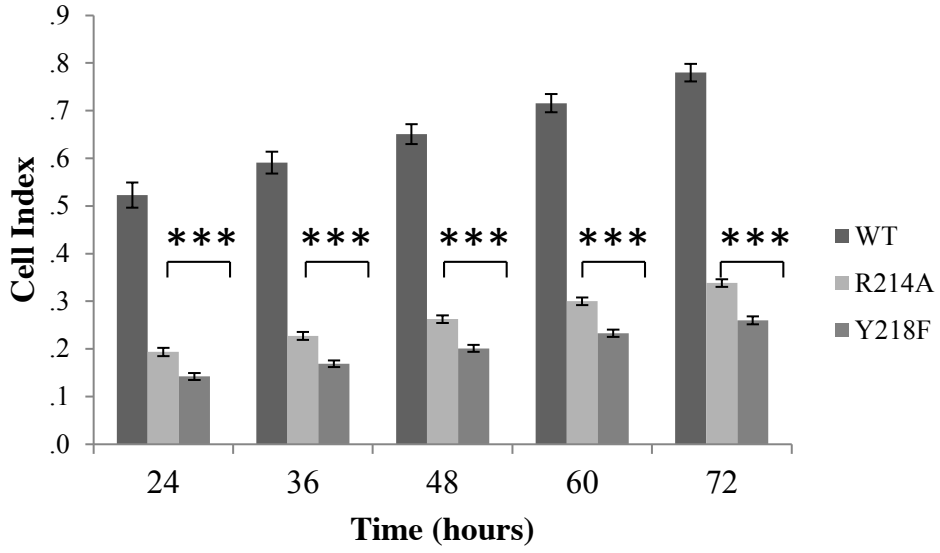

(iii)

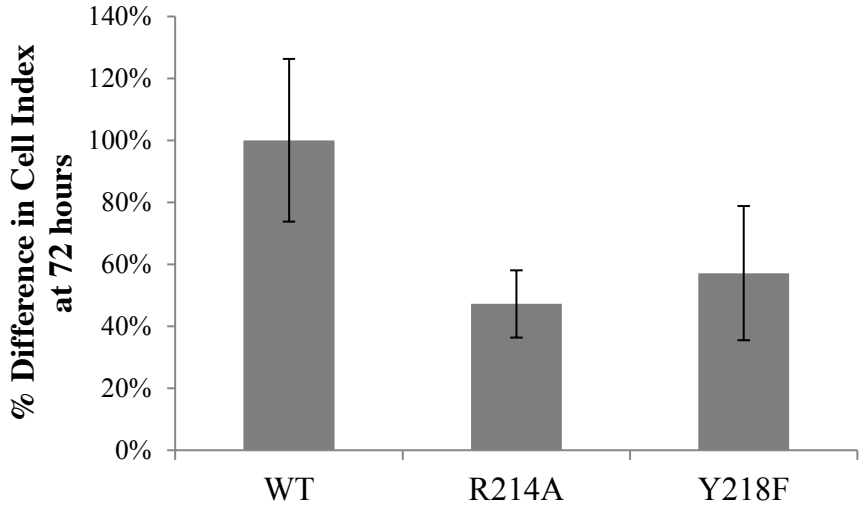

Figure 6

(a)

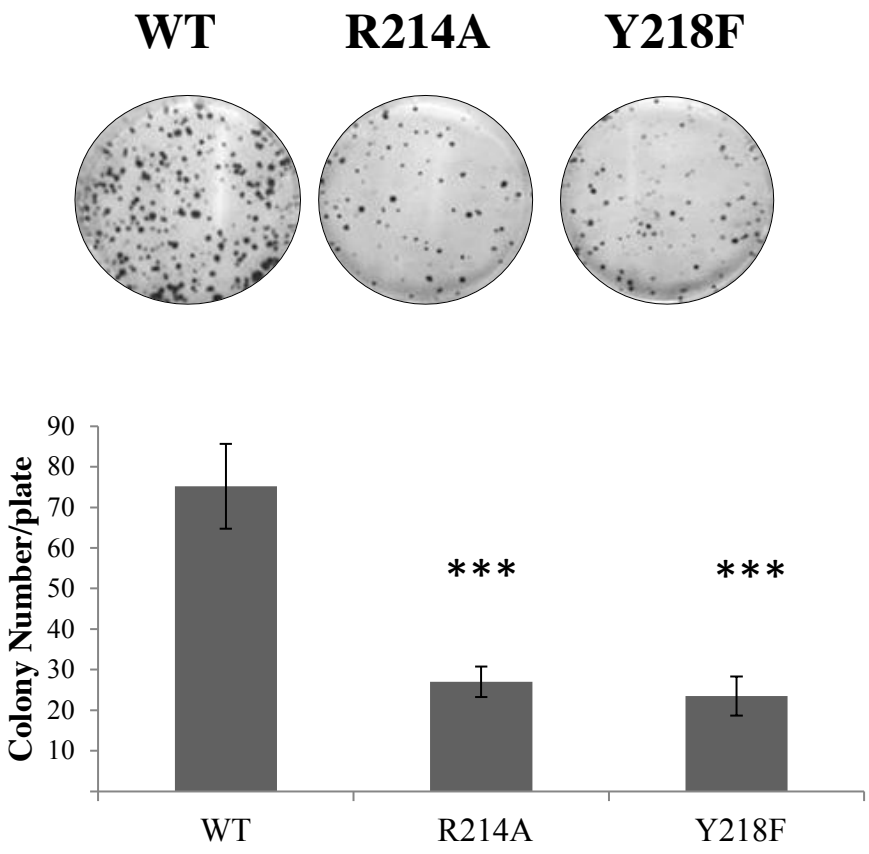
WT
R214A
Y218F
Colony Number/plate
90
80
70
60
50
40
30
20
10
***
***
WT
R214A
Y218F

(b)

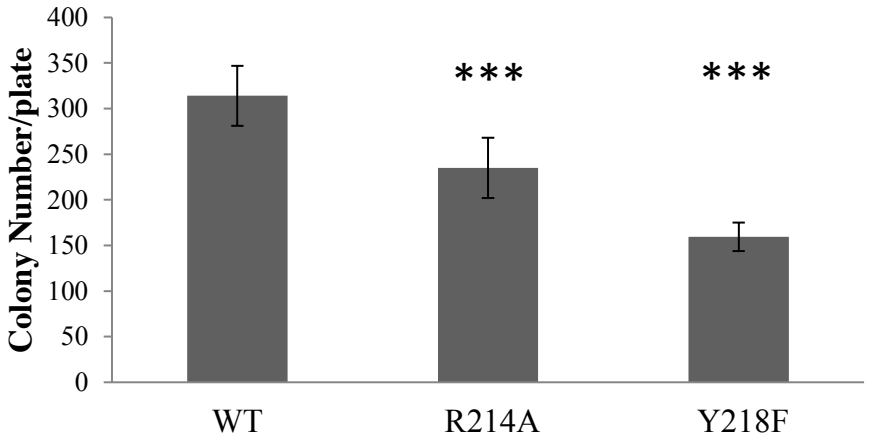
Colony Number/plate
400
350
300
250
200
150
100
50
0
***
***
WT
R214A
Y218F

Supplementary Figure 1

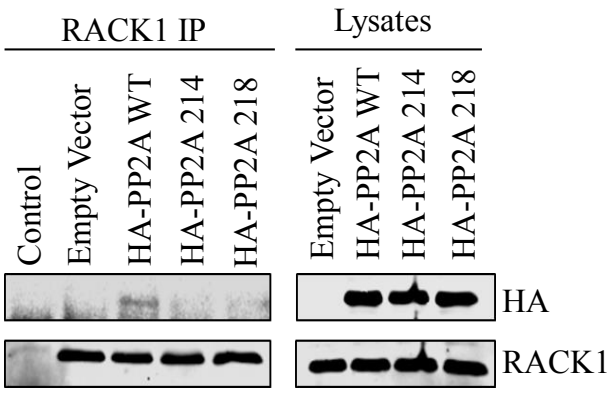

Supplementary Figure 2

(a)

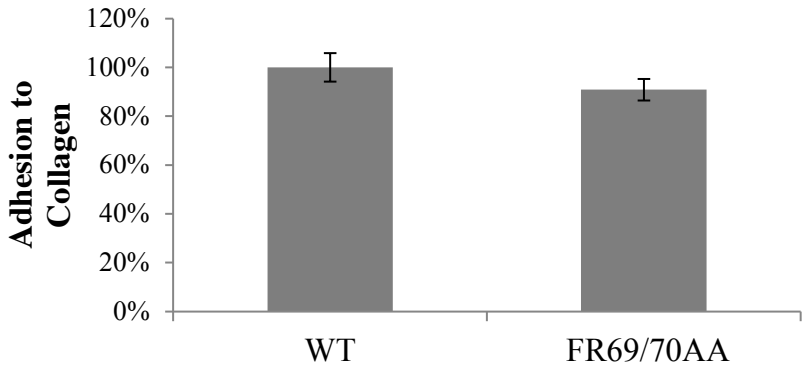

(b) (i)

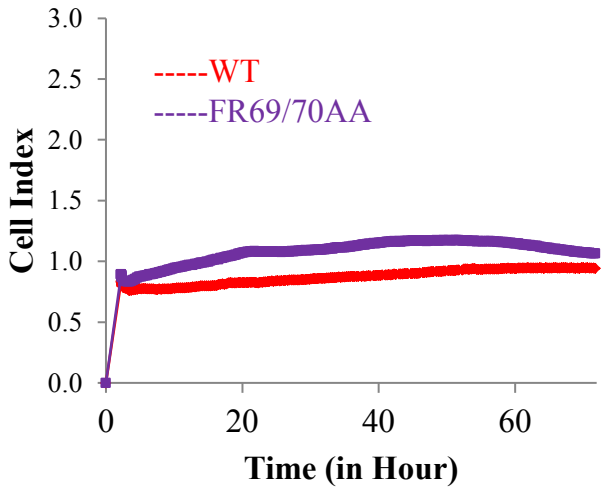

(ii)